Downloaded from jmg.bmj.com on April 17, 2014 - Published by group.bmj.com

Methods

Funding This project was funded by the Swedish Science Council, the Brain Research Foundation, Mr B Hållsten's Brain Research Foundation, The Ulla-Carin Lindquist's Fundation for ALS Research, the Knut and Alice Wallenberg Foundation, Swedish Brain Power, the European Community's Health Seventh Framework Programme (FP7/2007–2013) (grant agreement no. 259867), The Belgian Science Policy Office Interuniversity Attraction Poles (IAP) programme, the Flemish Government supported Europe Initiative on Centers of Excellence in Neurodegeneration (CoEN), the Flemish Government initiated Methusalem excellence research programme, Alzheimer Research Foundation, the Medical Foundation Queen Elisabeth, the Research Foundation Flanders (FWO) and the FWO provided a postdoctoral scientist fellowship to JvdZ, University of Antwerp Research Fund, the Swiss ALS Foundation, the Italian Ministry of Health (RF-2009-1473856), Grant-in-Aid for the Research Committee of CNS Degenerative Diseases and Comprehensive Research on Disability Health and Welfare from the Ministry of Health, Labour and Welfare in Japan and Dr Van Blitterswijk is supported by the Milton Safenowitz Post-Doctoral Fellowship for ALS research from the ALS Association.

Competing interests None.

Ethics approval The Medical Ethical Review Boards in Sweden, Switzerland and Portugal.

Provenance and peer review Not commissioned; externally peer reviewed.

Open Access This is an Open Access article distributed in accordance with the Creative Commons Attribution Non Commercial (CC BY-NC 3.0) license, which permits others to distribute, remix, adapt, build upon this work non-commercially, and license their derivative works on different terms, provided the original work is properly cited and the use is non-commercial. See: http://creativecommons.org/licenses/by-nc/3.0/

REFERENCES

1 DeJesus-Hernandez M, Mackenzie IR, Boeve BF, Boxer AL, Baker M, Rutherford NJ, Nicholson AM, Finch NA, Flynn H, Adamson J, Kouru N, Wojtas A, Sengdy P, Hsiung GY, Karydas A, Seeley WW, Josephs KA, Coppola G, Geschwind DH, Wszolek ZK, Feldman H, Knopman DS, Petersen RC, Miller BL, Dickson DW, Boylan KB, Graff-Radford NR, Rademakers R. Expanded GGGGCC hexanucleotide repeat in noncoding region of *C9ORF72* causes chromosome 9p-linked FTD and ALS. *Neuron* 2011;72:245–56.

2 Renton AE, Majounie E, Waite A, Simón-Sánchez J, Rollinson S, Gibbs JR, Schymick JC, Laaksovirta H, van Swieten JC, Myllykangas L, Kalimo H, Paetau A, Abramzon Y, Remes AM, Kaganovich A, Scholz SW, Duckworth J, Ding J, Harmer DW, Hernandez DG, Johnson JO, Mok K, Ryten M, Trabuni D, Guerreiri RJ, Orrell RW, Neal J, Murray A, Pearson J, Jansen IE, Sondervan D, Seelar H, Blake D, Young K, Halliwell N, Callister JB, Toulson G, Richardson A, Gerhard A, Snowden J, Mann D, Neary D, Nalls MA, Peuralinna T, Jansson L, Isoviita VM, Kaivorinne AL, Hölttä-Vuori M, Ikonen E, Sulkava R, Benatar M, Wuu J, Chiò A, Restagno G, Borghera G, Sabatelli M, ITALSGEN ConsortiumHeckerman D, Rogaeva E, Zinman L, Rothstein JD, Sendtner M, Drepper C, Eichler EE, Alkan C, Abdullaev Z, Pack SD, Dutra A, Pak E, Hardy J, Singleton A, Williams NM, Heutink P, Pickering-Brown S, Morris HR, Tienari PJ, Traynor BJ. A hexanucleotide repeat expansion in *C9ORF72* is the cause of chromosome 9p21-linked ALS-FTD. *Neuron* 2011;72:257–68.

3 Gijselinck I, Van Langenhove T, van der Zee J, Sleegers K, Philtjens S, Kleinberger G, Janssens J, Bettens K, van Cauwenberghe C, Pereson S, Engelborghs S, Sieben A, De Jonghe P, Vandenberghe R, Santens P, De Bleecker J, Maes G, Bäumer V, Dillen L, Joris G, Couijt I, Corsmit E, Elinck E, Van Dongen J, Vermeulen S, Van den Broeck M, Vaerenberg C, Mattheijssens M, Peeters K, Robberecht W, Cras P, Martin JJ, De Deyn PP, Cruts M, Van Broeckhoven C. A *C9orf72* promoter repeat expansion in a Flanders-Belgian cohort with disorders of the frontotemporal lobar degeneration-amyotrophic lateral sclerosis spectrum: a gene identification study. *Lancet Neurol* 2012;11:54–65.

4 Smith BN, Newhouse S, Shatunov A, Vance C, Topp S, Johnson L, Miller J, Lee Y, Troakes C, Scott KM, Jones A, Gray I, Wright J, Hortobágyi T, Al-Sarraj S, Rogeli B, Powell J, Lupton M, Lovestone S, Sapp PC, Weber M, Nestor PJ, Schelhaas HJ, Asbroek AA, Silani V, Gellera C, Taroni F, Ticconi N, Van Den Berg L, Veldink J, Van Damme P, Robberecht W, Shaw PJ, Kirby J, Pall H, Morrison KE, Morris A, de Belleroche J, Vianney de Jong JM, Baas F, Andersen PM, Landers J, Brown RH Jr, Weale ME, Al-Chalabi A, Shaw CE. The *C9ORF72* expansion mutation is a common cause of ALS+/-FTD in Europe and has a single founder. *Eur J Hum Genet* 2013;21:102–8.

5 Majounie E, Renton AE, Mok K, Dopper EG, Waite A, Rollinson S, Chio A, Restagno G, Nicolaou N, Simon-Sanchez J, van Swieten JC, Abramzon Y, Johnson JO, Sendtner M, Pamphlett R, Orrell RW, Mead S, Sidle KC, Houlden H, Rohrer JD, Morrison KE, Pall H, Talbot K, Ansorge O, Chromosome 9-ALS/FTD Consortium; French research network on FTLD/FTLD/ALS; ITALSGEN ConsortiumHernandez DG, Arepalli S, Sabatelli M, Mora G, Corbo M, Giannini F, Calvo A, Englund E, Borghero G, Floris GL, Remes AM, Laaksovirta H, McCluskey L, Trojanowski JQ, Van Deerlin VM, Schellenberg GD, Nalls MA, Drory VE, Lu CS, Yeh TH, Ishiura H, Takahashi Y, Tsuji S, Le Ber I, Brice A, Drepper C, Williams N, Kirby J, Shaw P, Hardy J, Tienari PJ, Heutink P, Morris HR, Pickering-Brown S, Traynor BJ. Frequency of the *C9orf72* hexanucleotide repeat expansion in patients with amyotrophic lateral sclerosis and frontotemporal dementia: a cross-sectional study. *Lancet Neurol* 2012;11:323–30.

6 Curtis-Cioffi KM, Rodrigueiro DA, Rodrigues VC, Cicarelli RM, Scarel-Caminaga RM. Comparison between the polymerase chain reaction-based screening and the Southern blot methods for identification of fragile X syndrome. *Genet Test Mol Biomarkers* 2012;16:1303–8.

7 Hantash FM, Goos DG, Tsao D, Quan F, Buller-Burckle A, Peng M, Jarvis M, Sun W, Strom CM. Qualitative assessment of FMR1 (CGG)n triplet repeat status in normal, intermediate, premutation, full mutation, and mosaic carriers in both sexes: implications for fragile X syndrome carrier and newborn screening. *Genet Med* 2010;12:162–73.

8 Beck J, Poulter M, Hensman D, Rohrer JD, Mahoney CJ, Adamson G, Campbell T, Uphill J, Borg A, Fratta P, Orrell RW, Malaspina A, Rowe J, Brown J, Hodges J, Sidle K, Polke JM, Houlden H, Schott JM, Fox NC, Rossor MN, Tabrizi SJ, Isaacs AM, Hardy J, Warren JD, Collinge J, Mead S. Large *C9orf72* hexanucleotide repeat expansions are seen in multiple neurodegenerative syndromes and are more frequent than expected in the UK population. *Am J Hum Genet* 2013;92:345–53.

9 Dobson-Stone C, Hallupp M, Loy CT, Thompson EM, Haan E, Sue CM, Panegyres PK, Razquin C, Seijo-Martínez M, Rene R, Gascon J, Campdelacreu J, Schmoll B, Volk AE, Brooks WS, Schofield PR, Pastor P, Kwok JB. *C9ORF72* repeat expansion in Australian and Spanish frontotemporal dementia patients. *PLoS ONE* 2013;8:e56899.

10 van Blitterswijk M, DeJesus-Hernandez M, Niemantsverdriet E, Murray ME, Heckman MG, Diehl NN, Brown PH, Baker MC, Finch NA, Bauer PO, Serrano G, Beach TG, Josephs KA, Knopman DS, Petersen RC, Boeve BF, Graff-Radford NR, Boylan KB, Petrucelli L, Dickson DW, Rademakers R. Association between repeat sizes and clinical and pathological characteristics in carriers of *C9ORF72* repeat expansions (Xpansize-72): a cross-sectional cohort study. *Lancet Neurol* 2013;12:978–88.

11 Andersen PM, Abrahams S, Borasio GD, de Carvalho M, Chio A, Van Damme P, Hardiman O, Kollewe K, Morrison KE, Petri S, Pradat PF, Silani V, Tomik B, Wasner M, Weber M. EFNS Task Force on Management of Amyotrophic Lateral Sclerosis. EFNS guidelines on the Clinical Management of Amyotrophic Lateral Sclerosis (MALS)—revised report of an EFNS task force. *Eur J Neurol* 2012;19:360–75.

12 Neary D, Snowden J, Mann D. Frontotemporal dementia. *Lancet Neurol* 2005;4:771–80.

13 van der Zee J, Gijselinck I, Dillen L, Van Langenhove T, Theuns J, Engelborghs S, Philtjens S, Vandenbulcke M, Sleegers K, Sieben A, Bäumer V, Maes G, Corsmit E, Borroni B, Padovani A, Archetti S, Perneczky R, Diehl-Schmid J, de Mendonça A, Miltenberger-Miltenyi G, Pereira S, Pimentel J, Nacmias B, Bagnoli S, Sorbi S, Graff C, Chiang HH, Westerlund M, Sanchez-Valle R, Llado A, Gelpi E, Santana I, Almeida MR, Santiago B, Frisoni G, Zanetti O, Bonvicini C, Synofzik M, Maetzler W, Vom Hagen JM, Schöls L, Heneka MT, Jessen F, Matej R, Parobkova E, Kovacs GG, Ströbel T, Sarafov S, Tournev I, Jordanova A, Danek A, Arzberger T, Fabrizi GM, Testi S, Salmon E, Santens P, Martin JJ, Cras P, Vandenberghe R, De Deyn PP, Cruts M, Van Broeckhoven C, van der Zee J, Gijselinck I, Dillen L, Van Langenhove T, Theuns J, Philtjens S, Sleegers K, Bäumer V, Maes G, Corsmit E, Engelborghs S, De Deyn PP, Cras P, Engelborghs S, De Deyn PP, Vandenbulcke M, Borroni B, Padovani A, Archetti S, Perneczky R, Diehl-Schmid J, Synofzik M, Maetzler W, Müller Vom Hagen J, Schöls L, Synofzik M, Maetzler W, Müller Vom Hagen J, Schöls L, Heneka MT, Jessen F, Ramirez A, Kurzwelly D, Sachtleben C, Mairer W, de Mendonça A, Miltenberger-Miltenyi G, Pereira S, Firmo C, Pimentel J, Sanchez-Valle R, Llado A, Antonell A, Molinuevo J, Gelpi E, Graff C, Chiang HH, Westerlund M, Graff C, Kinhult Ståhlbom A, Thonberg H, Nennesmo I, Börjesson-Hanson A, Nacmias B, Bagnoli S, Sorbi S, Bessi V, Piaceri I, Santana I, Santiago B, Santana I, Helena Ribeiro M, Rosário Almeida M, Oliveira C, Massano J, Garret C, Pires P, Frisoni G, Zanetti O, Bonvicini C, Sarafov S, Tournev I, Jordanova A, Tournev I, Kovacs GG, Ströbel T, Heneka MT, Jessen F, Ramirez A, Kurzwelly D, Sachtleben C, Mairer W, Jessen F, Matej R, Parobkova E, Danel A, Arzberger T, Maria Fabrizi G, Testi S, Ferrari S, Cavallaro T, Salmon E, Santens P, Cras P; European Early-Onset Dementia Consortium. A pan-European study of the *C9orf72* repeat associated with FTLD: geographic prevalence, genomic instability, and intermediate repeats. *Hum Mutat* 2013;34:363–73.

Wakabayashi *et al. Acta Neuropathologica Communications* 2014, **2**:173
http://www.actaneurocomms.org/content/2/1/173

ACTA NEUROPATHOLOGICA COMMUNICATIONS

RESEARCH Open Access

Analysis of microRNA from archived formalin-fixed paraffin-embedded specimens of amyotrophic lateral sclerosis

Koichi Wakabayashi[1*], Fumiaki Mori[1], Akiyoshi Kakita[2], Hitoshi Takahashi[3], Jun Utsumi[4] and Hidenao Sasaki[4]

Abstract

Background: MicroRNAs (miRNAs) are noncoding small RNAs that regulate gene expression. This study investigated whether formalin-fixed paraffin-embedded (FFPE) specimens from postmortem cases of neurodegenerative disorders would be suitable for miRNA profiling.

Results: Ten FFPE samples from 6 cases of amyotrophic lateral sclerosis (ALS) and 4 neurologically normal controls were selected for miRNA analysis on the basis of the following criteria for RNA quality: (i) a postmortem interval of less than 6 hours, (ii) a formalin fixation time of less than 4 weeks, (iii) an RNA yield per sample of more than 500 ng, and (iv) sufficient quality of the RNA agarose gel image. An overall RNA extraction success rate was 46.2%. For ALS, a total of 364 miRNAs were identified in the motor cortex, 91 being up-regulated and 233 down-regulated. Target genes were predicted using miRNA bioinformatics software, and the data applied to ontology analysis. This indicated that one of the miRNAs up-regulated in ALS (miR-338-3p) had already been identified in leukocytes, serum, cerebrospinal fluid and frozen spinal cord from ALS patients.

Conclusion: Although analysis was possible for just under half of the specimens examined, we were able to show that informative miRNA data can be derived from archived FFPE samples from postmortem cases of neurodegenerative disorders.

Keywords: AMBRA1, Amyotrophic lateral sclerosis, Autophagy, Bioinformatics, Formalin-fixed paraffin-embedded specimen, MicroRNA

Introduction

MicroRNAs (miRNAs) are small, single-stranded, non-coding RNAs that regulate gene expression at the transcriptional and translational levels in both plants and animals [1]. A single miRNA may bind to as many as 200 target genes [2]. miRNAs are of great interest because they can regulate approximately 30% of human genes [3] and have a huge impact on a wide range of basic biological processes including developmental timing, cell death, cell proliferation, hematopoiesis and patterning of the nervous system [4]. The implications of miRNA network dysregulation have already been well demonstrated in the field of cancer research, suggesting that miRNAs may be good biomarkers for cancer diagnosis and prognosis [5]. The role of miRNAs has also been studied in neurodegenerative conditions such as Alzheimer s disease [6-22], Parkinson s disease [19,23-27], Huntington s disease [28-30], multiple system atrophy [31] and amyotrophic lateral sclerosis (ALS) [19,32-36], postmortem frozen brain tissue having been employed in most cases [6-22,26,28,30,31]. Several investigators have also analyzed miRNAs from cerebrospinal fluid (CSF) [6,34,37], peripheral blood [33,34,37-39] and skeletal muscle [32,35].

Although the yield, quality and integrity of RNA can be reduced through cross-linking with proteins, enzyme degradation as well as chemical degradation during the fixation process [40-44], the expression of miRNAs in formalin-fixed paraffin-embedded (FFPE) samples is known to be well correlated with that in fresh frozen samples [45]. Moreover, the expression of miRNAs is preserved after routine fixation in formalin (up to 5 days)

* Correspondence: koichi@cc.hirosaki-u.ac.jp
[1]Department of Neuropathology, Institute of Brain Science, Hirosaki University Graduate School of Medicine, 5 Zaifu-cho, Hirosaki 036-8562, Japan
Full list of author information is available at the end of the article

BioMed Central

? 2014 Wakabayashi et al.; licensee BioMed Central. This is an Open Access article distributed under the terms of the Creative Commons Attribution License (http://creativecommons.org/licenses/by/4.0), which permits unrestricted use, distribution, and reproduction in any medium, provided the original work is properly credited. The Creative Commons Public Domain Dedication waiver (http://creativecommons.org/publicdomain/zero/1.0/) applies to the data made available in this article, unless otherwise stated.

and long-term storage in paraffin (up to 10 years) [45]. Therefore, FFPE samples have recently been used for studies of miRNA in cancer [46-51]. However, the stability and expression of miRNAs in FFPE specimens obtained postmortem and fixed for longer time periods (weeks or months) have not been investigated.

In the present study, we isolated RNAs from archived FFPE brain specimens of postmortem cases of ALS and neurologically normal controls. Although miRNA analysis was possible for only a minority of FFPE blocks, we were able to show that informative data can be derived from selected FFPE postmortem specimens of human brain.

Materials and methods

Subjects

To investigate the effect of postmortem interval, formalin fixation and storage period on the stability of RNA, we selected 10 samples (Table 1) that had been obtained at autopsy from 1 to 10 hours after death. The brains from which the specimens had been obtained had been immersed in 10% or 20% formalin or 10% phosphate-buffered formalin for 3 16 weeks. After fixation, the cerebrum had been cut into slices 10 mm thick in the coronal plane. Samples had then been removed from each slice and subjected to tissue processing (dehydration, clearing and impregnation) on an automated instrument (Tissue-Tek VIP 5 Jr., Sakura Finetek Japan, Tokyo, Japan) that employed seven steps of 100% ethanol, three steps of xylene, and four steps of paraffin, with 8 hours at each step. The instrument was operated under vacuum and heated to 37C for the ethanol and xylene steps and 60C for the paraffin steps. After tissue processing, each specimen had been embedded in paraffin, and the paraffin blocks had been stored for 10 86 months at room temperature protected from air and sunlight.

On the basis of the criteria reported by Osawa et al. [50], four criteria were adopted for establishing the suitability of the samples for RNA analysis: (i) a postmortem interval of less than 6 hours, (ii) a formalin fixation time of less than 4 weeks, (iii) a total RNA yield per sample of more than 500 ng, and (iv) sufficient quality of the RNA electrophoresis pattern.

We further evaluated an additional 16 samples (8 cases of ALS and 8 cases of normal controls) for which the postmortem interval had been less than 6 hours and the formalin fixation time had been less than 4 weeks. Thus, we evaluated a total of 26 samples. On this basis, 10 FFPE samples were selected for miRNA analysis, comprising 6 cases of sporadic ALS and 4 neurologically normal controls (Table 2). The FFPE specimens employed were from the motor cortex of patients with ALS and normal subjects. All the diagnoses had been confirmed by neuropathological examination using immunohistochemistry for TDP-43 and ubiquitin. This study was approved by the Institutional Ethics Committee of Hirosaki University Graduate School of Medicine, Japan.

RNA extraction

Two 5-μm-thick sections were cut from each block and placed in sterile 1.5-mL centrifuge tubes ready for extraction. Tubes containing cut FFPE sections for RNA purification were stored at −80C until use. Total RNA including small RNAs was extracted using an Arcturus Paradise PLUS FFPE RNA Isolation Kit (Life Technologies Corporation, Carlsbad, CA, USA) with the following modifications. Paraffin was removed by xylene treatment and the tissues were washed with ethanol twice to remove the xylene. The tissues were then treated with proteinase K at 37C overnight, as proteinase K enables extraction of almost the same amount of RNA from FFPE specimens as from fresh frozen samples [52]. After centrifugation, the supernatant was processed with a

Table 1 Summary of fixed paraffin-embedded samples used for RNA isolation

Sample no.	Pathological diagnosis	Postmortem interval (hours)	Fixation time (weeks)	Fixative	Storage period (months)	Sample size (mm)	RNA yield (ng)
1	ALS	1	4	20% F	24	30?40	3198
2	ALS	2	4	10% BF	49	30?40	4178
3	ALS	9	8	20% F	56	30?50	911
4	ALS	9	12	20% F	10	30?50	601
5	ALS	9	16	20% F	86	25?35	515
6	ALS	4	9	10% BF	24	20?25	594
7	ALS	4	10	10% BF	12	20?20	251
8	Control	4	4	10% F	38	30?40	2769
9	Control	10	3	10% F	86	25?40	1414
10	Control	10	4	10% F	64	30?45	765

ALS, amyotrophic lateral sclerosis, F, formalin, BF, buffered formalin.

Table 2 Characteristics of postmortem cases in microRNA study

Case no.	Pathological diagnosis	Age/gender	Disease duration (months)	Postmortem interval (hours)	Fixation time (weeks)	Storage period (months)
1	ALS	68/M	12	1	4	24
2	ALS	60/M	108	2	4	49
3	ALS	59/M	36	9	8	56
4	ALS	75/M	11	4	4	36
5	ALS	73/M	9	1.5	4	60
6	ALS	72/M	120	2	4	60
7	Control	67/F		4	4	38
8	Control	71/F		10	3	86
9	Control	84/M		10	4	64
10	Control	60/F		2	4	12

silica-based spin column (Toray Industries Inc., Tokyo, Japan) in order to obtain purified total RNA. The degrees of RNA cross-linking and RNA degradation were analyzed by agarose gel electrophoresis using an Agilent 2100 Bioanalyzer (Agilent Technologies, Santa Clara, CA, USA). RNA yield was determined from the A_{260}/A_{280} absorbance ratio using a NanoDrop ND-1000 spectrophotometer (Thermo Fisher Scientific, Waltham, MA, USA).

To assess the feasibility of analyzing RNA extracted from FFPE samples, we applied the selection criteria for RNA quality reported by Osawa et al. [50], as described above. The RNA electrophoresis pattern was found to be crucial for estimation of RNA quality. When the majority of RNAs were >4000 nucleotides (nt) in size due to cross-linking or when almost all of the RNAs were fragmented (e.g., <1000 nt), the RNA quality was considered unsuitable for miRNA analysis.

miRNA expression profiling

Extracted samples of total RNA that satisfied our criteria were labeled with Hy5 using a miRCURY LNA Array miR labeling kit (Exiqon, Vedbaek, Denmark). The labeled RNAs were then hybridized onto a 3D-Gene human miRNA oligo chip (Toray Industries Inc.). The annotation and oligonucleotide sequences of the probes conformed to the miRBase miRNA database Release 17v1.0.0 (http://www.mirbase.org/). After stringent washing, the fluorescent signals were scanned with a 3D-Gene Scanner (Toray Industries Inc.) and analyzed using 3D-Gene Extraction software (Toray Industries Inc.).

The raw data for each spot were normalized by subtraction of the mean intensity of the background signal determined from the signal intensities of all blank spots with 95% confidence intervals. Measurements for spots with signal intensities greater than 2 standard deviations (SD) of the background signal intensity were considered to be valid. The relative level of expression for a given miRNA was calculated by comparing the signal intensities of the valid spots throughout the microarray experiments. The normalized data were globally normalized per array, adjusting the median of the signal intensity to 25.

Any signal intensity level over 50 was considered to be significant. The signal was considered to be up-regulated when $\log_2 X$ was increased by 0.1 or more ($\geq \log_2 X = +0.1$) compared with the control signal level, and down-regulated when $\log_2 X$ was decreased by −0.1 or less ($\leq \log_2 X = -0.1$) compared with the control signal level.

miRNA targets and pathway analysis

Bioinformatics prediction of target genes and miRNA binding sites was performed using miRmap web-based open source software (http://mirmap.ezlab.org/) [53]. Canonical function and ontology analyses for candidate miRNA targets were performed using MetaCore Functional Analysis (ver.6.19, Thomson Reuter/GeneGo, http://lsresearch.thomsonreuters.com/) which is an integrated knowledge base and pathway analysis tool based on a proprietary manually curated database of human protein protein, protein DNA and protein compound interactions, and metabolic and signaling pathways, all supported by proprietary ontologies. Gene ontology enrichment analysis was also performed with Gene Ontology Consortium (GOC) web tool (http://geneontology.org/) to confirm standard GO term on the coincidences.

Immunohistochemistry

Since *SOGA1* (suppressor of glucose by autophagy) [54] was identified as one of the candidate target genes of both up-regulated and down-regulated miRNAs, we evaluated the protein expression levels of autophagy-related genes such as AMBRA1 [55], Beclin 1 [56], ULK1 [57] and ULK2 [57] using immunohistochemistry. Serial 4-μm-thick FFPE sections from the motor cortex and spinal cord (7th cervical, 8th thoracic and 4th lumbar segments) of ALS patients (n = 13) were employed. We also examined neurologically normal individuals (normal control) (n = 6)

and patients with various neurological diseases affecting the spinal anterior horn (diseased control) (n = 6). Three sections 40 μm apart were subjected to immunohistochemistry using the avidin-biotin-peroxidase complex method with a Vectastain ABC kit (Vector, Burlingame, CA, USA). The sections were subjected to heat retrieval using an autoclave for 10 min at 121C in 10 mM citrate buffer (pH 6.0), and then immunostained with rabbit polyclonal antibodies against AMBRA1 (NOVUS USA, Littleton, CO, USA; 1:1000), Beclin 1 (NOVUS USA; 1:200), ULK1 (Thermo Scientific, Rockford, IL, USA; 1:100) and ULK2 (Thermo Scientific; 1:500). Diaminobenzidine was used as the chromogen, and the sections were counterstained with hematoxylin.

Semi-quantitative analysis

Since AMBRA1 immunoreactivity was decreased in the spinal anterior horn cells in ALS, we assessed the number of AMBRA1-immunoreactive neurons in the spinal anterior horn of control subjects and patients with ALS using a semi-quantitative rating scale, as reported previously [58]: –, unstained; +, weakly stained; ++, moderately or intensely stained. In each case, the numbers of neurons were counted in Rexeds laminae VIII and IX of the lumbar spinal cord. Counting was performed at an original magnification of x200 using an eyepiece graticule and parallel sweeps of the microscope stage.

Statistical analysis

Calculations were performed using Statcel software (OMS Publishing, Tokorozawa, Japan). Repeated measures analysis of variance and Students or Welchs *t* test were used to evaluate possible differences in staining intensity between normal controls, diseased controls and ALS. Values were expressed as mean standard error of the mean. Correlations at $p < 0.05$ were considered to be significant.

Results

Stability of RNA in postmortem samples

The RNA yield was not correlated with the period of storage of FFPE blocks. However, the RNA yield was influenced by the period of formalin fixation (Table 1), being significantly higher in samples that had been fixed for a short period (3 4 weeks; mean 2465 ng) than in those that have been fixed for a long period (8 16 weeks; mean 574 ng) ($p < 0.05$). The RNA yield did not appear to be affected by the type of fixative employed. Postmortem interval could be also relevant. Samples with higher RNA yield (samples 1, 2 and 8) were the cases in whom postmortem interval was within 4 hours. The rest with lower RNA yield (samples 3 7, 9 and 10) had a combination of longer postmortem interval (9 10 hours) and/or fixation (8 16 weeks). RNA integrity was checked by electrophoresis, and a representative RNA agarose gel image is shown in Figure 1. A band of 5000 nt corresponding to 28S ribosomal RNA was slightly shifted toward a higher molecular weight in all cases, indicating overfixation with formalin and the presence of chemical modifications of the RNA such as covalently linked residual amino acids [59]. A band of 2000 nt corresponding to 18S ribosomal RNA was seen in some cases (Figure 1), suggesting that the extracted RNA was of good quality. These bands were not only shifted, but also appeared more diffuse and less focused. The bands of 100 200 nt corresponded to degraded RNA, as reported previously [60]. On the basis of these

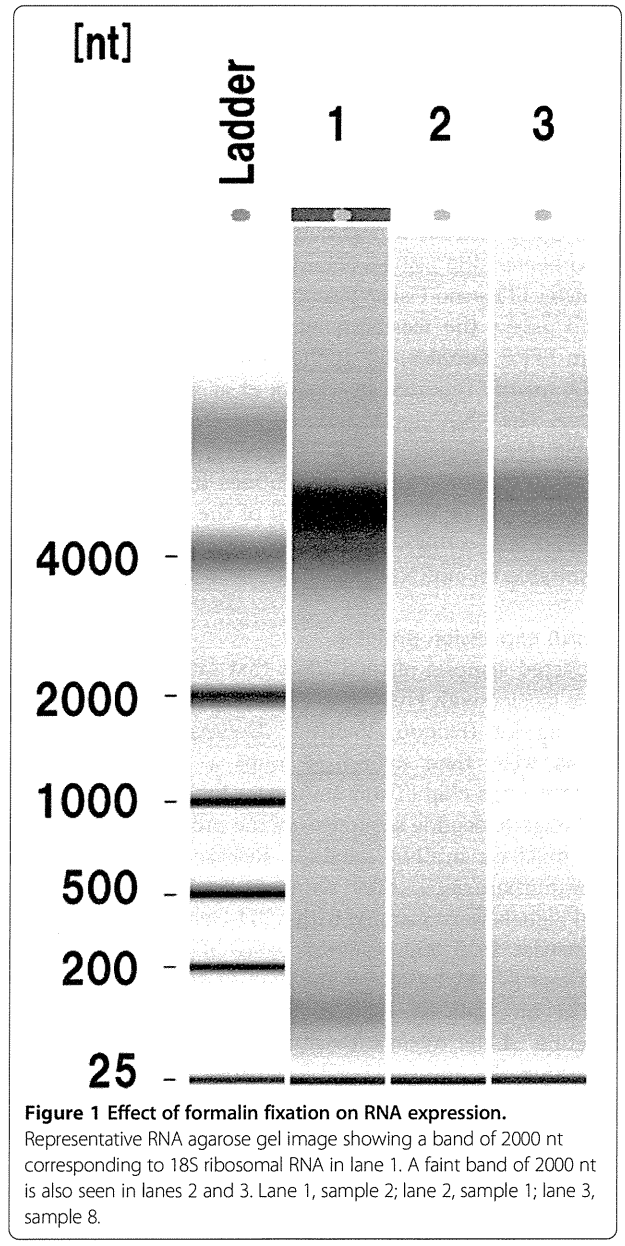

Figure 1 Effect of formalin fixation on RNA expression. Representative RNA agarose gel image showing a band of 2000 nt corresponding to 18S ribosomal RNA in lane 1. A faint band of 2000 nt is also seen in lanes 2 and 3. Lane 1, sample 2; lane 2, sample 1; lane 3, sample 8.

initial analyses, we adopted four criteria to indicate that RNA would be of sufficient quality for analysis, based on Osawa et al. [50]: (i) a postmortem interval of less than 6 hours, (ii) a formalin fixation time of less than 4 weeks, (iii) a total RNA yield per sample of more than 500 ng, and (iv) a RNA electrophoresis pattern of good quality.

We evaluated an additional 16 samples (8 cases of ALS and 8 cases of normal controls) for which the postmortem interval had been less than 6 hours and the formalin fixation time had been less than 4 weeks. The RNA yield was more than 500 ng for 12 of these samples, and the RNA agarose gel image was of sufficient quality in 4. As a result, we evaluated a total of 26 samples. The RNA yield was more than 500 ng in 20 of the 26 samples, and the RNA agarose gel image was of sufficient quality in 12. Thus, the success rate for analysis of RNA from FFPE samples of the human postmortem brain was 46.2% (12 of 26).

Based on the above step, 10 cases were selected for miRNA analysis; these included cases of sporadic ALS (n = 6) and neurologically normal controls (n = 4) (Table 2). In case 3, although the fixation time had been 8 weeks, it was included in the present analysis, because the RNA yield was more than 500 ng and the RNA agarose gel image was of sufficient quality.

miRNA analysis and candidate target genes in ALS

A total of 364 miRNAs were isolated from the motor cortex of patients with ALS. Forty miRNAs showed no change ($-0.1 < \log_2 X < +0.1$), and 91 were up-regulated ($\log_2 X \geqq +0.1$) and 233 were down-regulated ($\log_2 X \leqq -0.1$) relative to the controls. Top 20 microRNAs up- or down-regulated in ALS are shown in Additional file 1: Table S1. miR-494 was found to be the most highly differentially up-regulated miRNA (+4.99-fold change), followed in order by miR-4257, miR-24-3p, miR-4299, and miR-1973 as the top 5 up-regulated miRNAs. On the other hand, miR-4740-5p (+0.19-fold change), miR-1290, miR-3619-3p, miR-1246, and miR-3180-3p were the top 5 down-regulated miRNAs.

Scatter plot of all 364 miRNAs comparing signal intensity versus $\log_2$ fold-change of ALS/control ratio is shown in Figure 2. We selected 6 up-regulated miRNAs (miR-494, miR-4257, miR-24-3p, miR-4299, miR-1973 and miR-4485) and 8 down-regulated miRNAs (miR-4740-5p, miR-1290, miR-3619-3p, miR-1246, miR-3180-3p, miR-4648, miR-4716-3p and miR-663) in ALS. The candidate target genes of the 6 up-regulated and 8 down-regulated miRNAs in ALS were identified using miRmap web-based open source software.

Top 50 candidate target genes of each of the 6 up-regulated miRNAs in ALS were selected according to the miRmap score. Of the 300 target candidates identified for each of the 6 miRNAs, there was an overlap of 13 genes (Additional file 2: Table S2). These 13 genes have been reported to be involved in muscular cell proliferation (FOXK1 [61], MEF2D [62]), synaptic transmission (ITSN1 [63], RAB3B [64], SLC6A5 [65]), mitochondrial regulation (IBA57 [66], PPARGC1B [67]) and autophagy (MEF2D [68], SOGA1 [54]). These genes may be down-regulated by the 6 up-regulated miRNAs in affected brain regions of ALS. In addition, miR-24-3p showed the most matching frequency (7 overlapped in 50 targets) in up-regulated miRNAs.

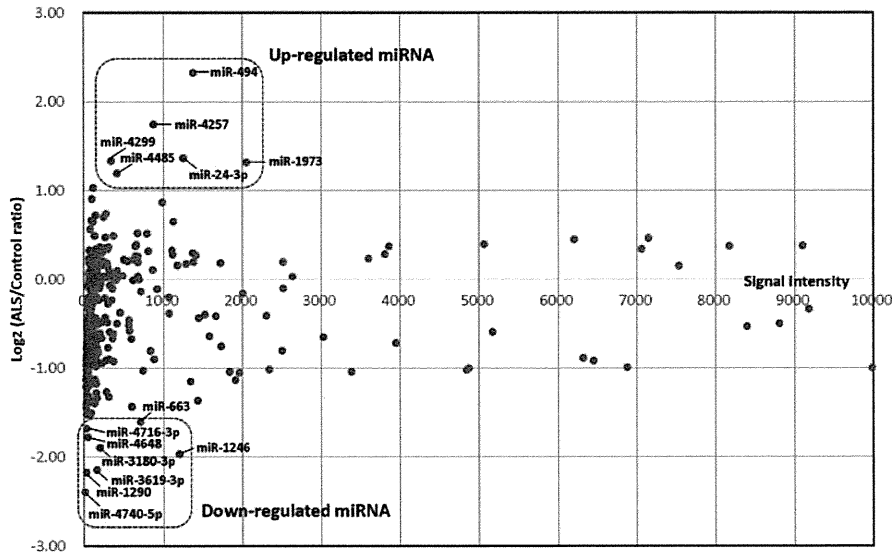

Figure 2 Scatter plot of all 364 miRNAs comparing signal intensity (X-axis) versus $\log_2$ fold-change of amyotrophic lateral sclerosis (ALS)/control ratio (Y-axis). Based on the size of variation, 6 up-regulated and 8 down-regulated miRNAs were selected in ALS.

Top 50 candidate target genes of each of the 8 down-regulated miRNAs in ALS were also selected. Of the 400 target candidates identified for each of the 8 miRNAs, there was an overlap of 34 genes (Additional file 3: Table S3). These 34 genes have been reported to play a role in neurogenesis (ONECUT2 [69], KDM5A [70], NAT8L [71], NFIX [72]), mitochondrial regulation (IBA57 [66]) and autophagy (PRLA [73], SNCB [74], SOGA1 [54]). In addition, miR-3180-3p showed the most matching frequency (14 overlapped in 50 targets) in down-regulated miRNAs.

It is important to note that 3 genes (*IBA57*, *RAB3B* and *SOGA1*) were identified as candidate target genes of both up-regulated and down-regulated miRNAs (Additional file 2: Table S2, Additional file 3: Table S3). *IBA57* is known to be involved in the biosynthesis of mitochondrial [4Fe-4S] proteins [66]. Mutation of *IBA57* causes severe myopathy and encephalopathy [66]. Rab3B is a synaptic vesicle protein that interacts with the Rab3-interacting molecule isoforms as effector proteins in a GTP-dependent manner [64]. The search for an inhibitor of autophagy in the adiponectin signaling pathway led to the discovery of the Suppressor of Glucose from Autophagy (SOGA) [54]. These findings suggest that mitochondrial regulation, synaptic transmission and autophagy may be affected in ALS. Considering that the expression level of up-regulated miRNAs is higher than that of down-regulated miRNAs (Figure 2), these 3 genes may be down-regulated in the motor cortex of ALS.

Gene ontology analysis of predicted target genes for disease-specific miRNAs

A total of 300 candidates for 6 up-regulated miRNAs and 400 candidates for 8 down-regulated miRNAs were nominated as targets for gene ontology enrichment analysis (biological process). Additional file 4: Table S4 (A, B) shows top 10 GO terms with MetaCore analysis and Additional file 4: Table S4 (C, D) shows top 10 GO terms with GOC analysis for standard GO terms. Two GO analyses suggested essentially similar biological process in up-regulated and down-regulated miRNA target genes.

The biological processes in ALS altered by these target genes were shown to be related to protein transport, synaptic vesicle-mediated transport, and localization for up-regulated miRNAs and nervous system development for down-regulated miRNAs, as shown in Additional file 4: Table S4.

Decrease of AMBRA1 immunoreactivity in ALS

Since *SOGA1* was identified as one of the overlapped target genes predicted by 6 up-regulated and 8 down-regulated miRNAs, we hypothesized that alteration of autophagy is involved in the disease process of ALS. This may be supported by the findings that abnormal autophagy is involved in various neurodegenerative disorders, including ALS [75-79]. Therefore, we evaluated the protein expression levels of autophagy-related genes such as AMBRA1 [55], Beclin 1 [56], ULK1 [57] and ULK2 [57] by immunohistochemical examination of FFPE tissue.

In specimens from normal control subjects, anti-AMBRA1 antibody strongly immunolabeled the cytoplasm of upper and lower motor neurons in a diffuse granular pattern (Figure 3A-C), consistent with a previous study [80]. In ALS, AMBRA1 immunoreactivity was decreased in the majority of spinal anterior horn cells (Figure 3D-F), but not in the motor cortex (data not shown), in comparison with controls.

Semi-quantitative analysis of normal controls showed that 30.2% of anterior horn cells were moderately or intensely immunolabeled, 48.5% were weakly immunolabeled, and 21.3% were unstained (Figure 4). Similarly, in diseased controls, 20% of anterior horn cells were moderately or intensely immunolabeled and 33.7% were weakly immunolabeled (Figure 4). The differences in staining intensity between normal and diseased controls were not statistically significant. In ALS, a small proportion of anterior horn cells (5.2%) showed moderate or intense immunoreactivity, whereas the majority (83.5%) were unstained (Figure 4). The differences in staining intensity between normal control and ALS cases and between diseased control and ALS cases were significant.

Immunoreactivity for Beclin 1, ULK1 and ULK2 was observed in the neuronal cytoplasm in normal controls. No significant difference was found in the staining intensity of these proteins between ALS and normal controls (data not shown).

Discussion

It has been reported that the formalin fixation and paraffin embedding process results in a marked reduction of detectable mRNA [81]. This process causes enzymatic degradation and chemical modification of RNA giving rise to cross-links with proteins and making RNA extraction difficult [52]. Therefore, a digestion step with proteinase K is required to eliminate cross-links and facilitate RNA extraction from FFPE samples [52]. The longer an RNA molecule is, the more likely cross-links will remain after proteinase K digestion, hence small RNA molecules will be easier to extract from FFPE samples and fragments larger than 200 nt will be harder to recover from FFPE samples. In addition, electrophoretic profiles of total RNA from frozen samples show three characteristic peaks: 40 80 nt, 90 nt and 150 nt, probably corresponding to tRNAs, rRNAs and snoRNAs, respectively. On the other hand, FFPE sample shows an accumulation of RNA fragments smaller than 200 nt [82]. These findings suggest that the amount of total RNA that can be extracted from a FFPE tissue sample is

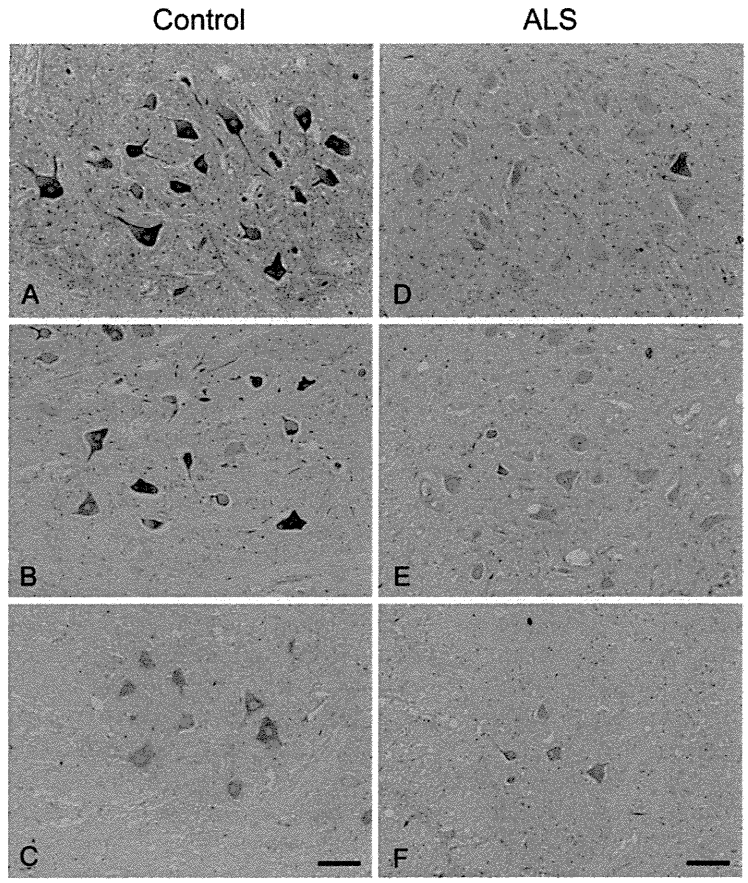

Figure 3 AMBRA1 immunoreactivity in the anterior horn of the lumbar cord in 3 normal controls (A-C) and 3 cases of ALS (D-F). AMBRA1 immunoreactivity is decreased in ALS relative to the controls. Bars = 100 μm.

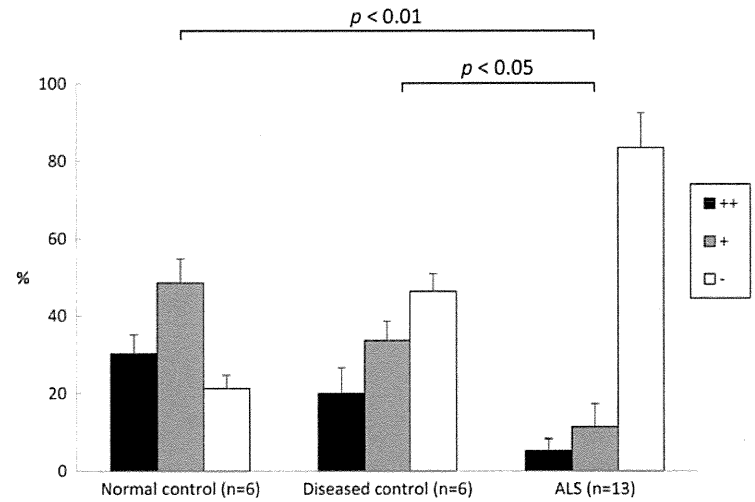

Figure 4 AMBRA1 immunoreactivity in anterior horn cells from normal and diseased controls and patients with ALS. The proportions of neurons showing intense/moderate (++, black column), weak (+, gray column), or no immunostaining for AMBRA1 (–, white column) relative to the total number of neurons in the anterior horn are indicated.

only a fraction of what can be extracted from its corresponding frozen tissue [81].

Although the number of subjects was small, we demonstrated for the first time that miRNAs extracted from FFPE samples of postmortem brain tissue from patients with neurodegenerative disorder (ALS) and neurologically normal controls were relatively well preserved; 12 of 26 samples (46.2%), for which the longest storage period was more than 7 years, provided RNA of sufficient quality. Thus, miRNAs appear to be relatively stable in FFPE samples, even those from postmortem specimens. It has been suggested that miRNAs are too small to be degraded [83]. However, this hypothesis has not been supported by any reported data. It is now known that active, mature miRNAs are processed and function via binding to Argonaute family proteins [84,85]. These protein-miRNA complexes may protect the functional population of miRNA from degradation, especially during the process of formalin fixation and storage in paraffin [49]. Peir-Chova et al. [82] have shown that the quantity of miRNAs from FFPE samples was higher than that obtained from frozen samples, since degradation of total RNA can produce fragments in the small RNA size range that could cause an overestimation in the proportion of its small sized fragments.

ALS is characterized by loss of upper and lower motor neurons. TDP-43 is now known to be a major component of ubiquitinated inclusions in ALS and frontotemporal lobar degeneration with ubiquitinated inclusions (FTLD-U, since renamed FTLD-TDP) [86,87]. Thus, these neurodegenerative disorders comprise a new disease concept: TDP-43 proteinopathy . Up- or down-regulated miRNAs in ALS in the present study and previously reported results are shown in Additional file 5: Table S5. Williams et al. [36] compared miRNA expression in skeletal muscle of normal and ALS model mice (G93A-SOD1 transgenic mice) and demonstrated that miR-206, a skeletal muscle-specific miRNA in humans and mice, delays disease progression in SOD1 transgenic mice. miR-206 is up-regulated in the skeletal muscle of ALS patients [32]. Shioya et al. [19] studied the miRNA expression profile in frozen samples of frontal cortex from three ALS patients using microarray analysis and found that miR-29a, miR-29b and miR-338-3p were up-regulated. Up-regulation of miR-29b has also been reported in skeletal muscle of ALS patients [35]. De Felice et al. [33] evaluated miRNA expression in leukocytes obtained from ALS patients and healthy controls and demonstrated that miR-338-3p was also up-regulated in ALS. Seven miRNAs (miR-451, miR-1275, miR-328, miR-638, miR-149, miR-665 and miR-583) were also down-regulated in ALS. Importantly, in our present study, three miRNAs (miR-29a, miR-29b and miR-338-3p) were also up-regulated and four miRNAs (miR-328, miR-451, miR-638 and miR-665) were down-regulated in FFPE samples of the motor cortex in ALS. Recently, De Felice et al. [34] further demonstrated that miR-338-3p was over-expressed in leukocytes, serum, CSF and frozen samples of spinal cord in patients with ALS, and that miR-338-3p expression in leukocytes was correlated with disease duration, suggesting that miR-338-3p may be a relevant clinical biomarker of ALS. It is likely that some miRNAs are systemically dysregulated in ALS and that miRNAs remain stable even in FFPE postmortem samples that have been stored for a long period.

We further demonstrated that AMBRA1 was significantly down-regulated in the lower motor neurons in ALS. This is in line with the results of our miRNA analysis that AMBRA1 is most possibly regulated by miR-24-3p according to miRmap prediction (the rank 1 in canonical miRNAs of miRmap score = 97.37) and that miR-24-3p is one of the highly up-regulated miRNAs in ALS (Additional file 1: Table S1). AMBRA1 is widely expressed in neurons in the normal mouse brain and is localized to the endoplasmic reticulum, perinuclear cisternae and outer mitochondrial membrane [80]. AMBRA1 interacts with Beclin 1, promoting its binding to lipid kinase Vps34, thus mediating autophagosome nucleation [55]. AMBRA1 is also known to be a Parkin-binding protein involved in mitophagy [88]. Abnormal autophagy is involved in various neurodegenerative disorders, including Alzheimer s disease [75,76], Parkinson s disease [78], multiple system atrophy [79] and ALS [77]. A recent study has shown that administration of rapamycin, an MTOR-dependent autophagy activator, ameliorates neuronal degeneration in FTLD-TDP model mice [89]. By contrast, rapamycin also aggravates neuronal death in a mouse model of ALS [90]. Thus, induction or repression of autophagy should be taken into account when considering novel therapeutic approaches for TDP-43 proteinopathy.

Conclusion

In conclusion, we have utilized FFPE brain samples from postmortem cases of ALS and neurologically normal controls and found that miRNAs extracted from these samples were relatively well preserved. Although further studies with a larger sample size are necessary, it is likely that archived FFPE postmortem samples can be a valuable source for miRNA profiling in neurodegenerative disorders.

Additional files

Additional file 1: Table S1. Top 20 microRNAs up- or down-regulated in the motor cortex in ALS.

Additional file 2: Table S2. Predicted target genes for ALS-specific up-regulated miRNAs identified by miRmap web-based open source software.

Additional file 3: Table S3. Predicted target genes for ALS-specific down-regulated miRNAs identified by miRmap web-based open source software.

Additional file 4: Table S4. Gene ontology enrichment analysis (bilogical process) of predicted target genes for disease-specific miRNAs.

Additional file 5: Table S5. Summary of up- or down-regulated miRNAs in ALS.

Competing interests
The authors declare that they have no competing interests.

Authors contributions
JU, HS and KW managed the study and were principally responsible for writing. FM, AK, HT and KW performed the neuropathological observation and evaluation. JU performed bioinformatics analysis. HS and KW supervised whole process of the study. All authors read and approved the final manuscript.

Acknowledgements
The authors wish to express their gratitude to M. Nakata, A. Ono and Y. Hama for technical assistance.

Funding
This work was supported by JSPS KAKENHI Grant Number 26430049 (F.M.) and 24300131 (K.W.), a Grant from Japan Science and Technology Program (AS2314204F) (H.S., K.W.), a Grant for Hirosaki University Institutional Research (K.W.), the Collaborative Research Project (2014 2508) of the Brain Research Institute, Niigata University (F.M.), Grants-in-Aid for Research on rare and intractable diseases, the Research Committee on Establishment of Novel Treatments for Amyotrophic Lateral Sclerosis (H.S.), the Research Committee for Ataxic Disease (H.S., K.W.) and the Research Committee of CNS Degenerative Diseases (H.S.) from the Ministry of Health, Labour and Welfare, Japan, and an Intramural Research Grant (24 5) for Neurological and Psychiatric Disorders of NCNP (K.W.).

Author details
[1]Department of Neuropathology, Institute of Brain Science, Hirosaki University Graduate School of Medicine, 5 Zaifu-cho, Hirosaki 036-8562, Japan. [2]Department of Pathological Neuroscience, Center for Bioresource-based Researches, Brain Research Institute, University of Niigata, Niigata, Japan. [3]Department of Pathology, Brain Research Institute, University of Niigata, Niigata, Japan. [4]Department of Neurology, Hokkaido University Graduate School of Medicine, Sapporo, Japan.

Received: 30 October 2014 Accepted: 1 December 2014
Published online: 14 December 2014

References
1. Bartel DP (2004) MicroRNAs: genomics, biogenesis, mechanism, and function. Cell 116(2):281 297
2. Esquela-Kerscher A, Slack FJ (2006) Oncomirs - microRNAs with a role in cancer. Nat Rev Cancer 6(4):259 269
3. Lewis BP, Burge CB, Bartel DP (2005) Conserved seed pairing, often flanked by adenosines, indicates that thousands of human genes are microRNA targets. Cell 120(1):15 20
4. Ambros V (2004) The functions of animal microRNAs. Nature 431(7006):350 355
5. Ma L, Weinberg RA (2008) Micromanagers of malignancy: role of microRNAs in regulating metastasis. Trends Genet 24(9):448 456
6. Cogswell JP, Ward J, Taylor IA, Waters M, Shi Y, Cannon B, Kelnar K, Kemppainen J, Brown D, Chen C, Prinjha RK, Richardson JC, Saunders AM, Roses AD, Richards CA (2008) Identification of miRNA changes in Alzheimer s disease brain and CSF yields putative biomarkers and insights into disease pathways. J Alzheimer s Dis 14(1):27 41
7. Cui JG, Li YY, Zhao Y, Bhattacharjee S, Lukiw WJ (2010) Differential regulation of interleukin-1 receptor-associated kinase-1 (IRAK-1) and IRAK-2 by microRNA-146a and NF-κB in stressed human astroglial cells and in Alzheimer disease. J Biol Chem 285(50):38951 38960
8. Faghihi MA, Zhang M, Huang J, Modarresi F, Van der Brug MP, Nalls MA, Cookson MR, St-Laurent G 3rd, Wahlestedt C (2010) Evidence for natural antisense transcript-mediated inhibition of microRNA function. Genome Biol 11(5):R56
9. Geekiyanage H, Chan C (2011) MicroRNA-137/181c regulates serine palmitoyltransferase and in turn amyloid β, novel targets in sporadic Alzheimer s disease. J Neurosci 31(41):14820 14830
10. G?tz J, Ittner LM, F?ndrich M, Schonrock N (2008) Is tau aggregation toxic or protective: a sensible question in the absence of sensitive methods? J Alzheimer s Dis 14(4):423 429
11. H?bert SS, Horr? K, Nicola? L, Papadopoulou AS, Mandemakers W, Silahtaroglu AN, Kauppinen S, Delacourte A, De Strooper B (2008) Loss of microRNA cluster miR-29a/b-1 in sporadic Alzheimer s disease correlates with increased BACE1/β-secretase expression. Proc Natl Acad Sci U S A 105(17):6415 6420
12. H?bert SS, Horr? K, Nicola? L, Bergmans B, Papadopoulou AS, Delacourte A, De Strooper B (2009) MicroRNA regulation of Alzheimer s amyloid precursor protein expression. Neurobiol Dis 33(3):422 428
13. H?bert SS, Papadopoulou AS, Smith P, Galas MC, Planel E, Silahtaroglu AN, Sergeant N, Bu?e L, De Strooper B (2010) Genetic ablation of Dicer in adult forebrain neurons results in abnormal tau hyperphosphorylation and neurodegeneration. Hum Mol Genet 19(20):3959 3969
14. Lukiw WJ (2007) Micro-RNA speciation in fetal, adult and Alzheimer s disease hippocampus. Neuroreport 18(3):297 300
15. Lukiw WJ, Zhao Y, Cui JG (2008) An NF-κB-sensitive micro RNA-146a-mediated inflammatory circuit in Alzheimer disease and in stressed human brain cells. J Biol Chem 283(46):31315 31322
16. Nunez-Iglesias J, Liu CC, Morgan TE, Finch CE, Zhou XJ (2010) Joint genome-wide profiling of miRNA and mRNA expression in Alzheimer s disease cortex reveals altered miRNA regulation. PLoS One 5(2):e8898
17. Schratt G (2009) microRNAs at the synapse. Nat Rev Neurosci 10(12):842 849
18. Sethi P, Lukiw WJ (2009) Micro-RNA abundance and stability in human brain: specific alterations in Alzheimer s disease temporal lobe neocortex. Neurosci Lett 459(2):100 104
19. Shioya M, Obayashi S, Tabunoki H, Arima K, Saito Y, Ishida T, Satoh J (2010) Aberrant microRNA expression in the brains of neurodegenerative diseases: miR-29a decreased in Alzheimer disease brains targets neurone navigator 3. Neuropathol Appl Neurobiol 36(4):320 330
20. Smith P, Al Hashimi A, Girard J, Delay C, H?bert SS (2011) In vivo regulation of amyloid precursor protein neuronal splicing by microRNAs. J Neurochem 116(2):240 247
21. Wang WX, Rajeev BW, Stromberg AJ, Ren N, Tang G, Huang Q, Rigoutsos I, Nelson PT (2008) The expression of microRNA miR-107 decreases early in Alzheimer s disease and may accelerate disease progression through regulation of β-site amyloid precursor protein-cleaving enzyme 1. J Neurosci 28(5):1213 1223
22. Wang WX, Huang Q, Hu Y, Stromberg AJ, Nelson PT (2011) Patterns of microRNA expression in normal and early Alzheimer s disease human temporal cortex: white matter versus gray matter. Acta Neuropathol 121(2):193 205
23. Doxakis E (2010) Post-transcriptional regulation of α-synuclein expression by mir-7 and mir-153. J Biol Chem 285(17):12726 12734
24. Gehrke S, Imai Y, Sokol N, Lu B (2010) Pathogenic LRRK2 negatively regulates microRNA-mediated translational repression. Nature 466(7306):637 641
25. Junn E, Lee KW, Jeong BS, Chan TW, Im JY, Mouradian MM (2009) Repression of alpha-synuclein expression and toxicity by microRNA-7. Proc Natl Acad Sci U S A 106(31):13052 13057
26. Kim J, Inoue K, Ishii J, Vanti WB, Voronov SV, Murchison E, Hannon G, Abeliovich A (2007) A microRNA feedback circuit in midbrain dopamine neurons. Science 317(5842):1220 1224
27. Wang G, van der Walt JM, Mayhew G, Li YJ, Z?chner S, Scott WK, Martin ER, Vance JM (2008) Variation in the miRNA-433 binding site of FGF20 confers risk for Parkinson disease by overexpression of α-synuclein. Am J Hum Genet 82(2):283 289
28. Johnson R, Zuccato C, Belyaev ND, Guest DJ, Cattaneo E, Buckley NJ (2008) A microRNA-based gene dysregulation pathway in Huntington s disease. Neurobiol Dis 29(3):438 445
29. Lee ST, Chu K, Im WS, Yoon HJ, Im JY, Park JE, Park KH, Jung KH, Lee SK, Kim M, Roh JK (2011) Altered microRNA regulation in Huntington s disease models. Exp Neurol 227(1):172 179
30. Packer AN, Xing Y, Harper SQ, Jones L, Davidson BL (2008) The bifunctional microRNA miR-9/miR-9* regulates REST and CoREST and is downregulated in Huntington s disease. J Neurosci 28(53):14341 14346
31. Ubhi K, Rockenstein E, Kragh C, Inglis C, Spencer B, Michael S, Mante M, Adame A, Galasko D, Masliah E (2014) Widespread microRNA dysregulation

in multiple system atrophy - disease-related alteration in miR-96. Eur J Neurosci 39(6):1026 1041
32. Bruneteau G, Simonet T, Bauch? S, Mandjee N, Malfatti E, Girard E, Tanguy ML, Behin A, Khiami F, Sariali E, Hell-Remy C, Salachas F, Pradat PF, Fournier E, Lacomblez L, Koenig J, Romero NB, Fontaine B, Meininger V, Schaeffer L, Hanta? D (2013) Muscle histone deacetylase 4 upregulation in amyotrophic lateral sclerosis: potential role in reinnervation ability and disease progression. Brain 136(Pt 8):2359 2368
33. De Felice B, Guida M, Guida M, Coppola C, De Mieri G, Cotrufo R (2012) A miRNA signature in leukocytes from sporadic amyotrophic lateral sclerosis. Gene 508(1):35 40
34. De Felice B, Annunziata A, Fiorentino G, Borra M, Biffali E, Coppola C, Cotrufo R, Brettschneider J, Giordana ML, Dalmay T, Wheeler G, D Alessandro R (2014) miR-338-3p is over-expressed in blood, CFS, serum and spinal cord from sporadic amyotrophic lateral sclerosis patients. Neurogenetics: Epub ahead of print
35. Russell AP, Wada S, Vergani L, Hock MB, Lamon S, L?ger B, Ushida T, Cartoni R, Wadley GD, Hespel P, Kralli A, Soraru G, Angelini C, Akimoto T (2012) Disruption of skeletal muscle mitochondrial network genes and miRNAs in amyotrophic lateral sclerosis. Neurobiol Dis 49C:107 117
36. Williams AH, Valdez G, Moresi V, Qi X, McAnally J, Elliott JL, Bassel-Duby R, Sanes JR, Olson EN (2009) MicroRNA-206 delays ALS progression and promotes regeneration of neuromuscular synapses in mice. Science 326 (5959):1549 1554
37. Freischmidt A, M?ller K, Ludolph AC, Weishaupt JH (2013) Systemic dysregulation of TDP-43 binding microRNAs in amyotrophic lateral sclerosis. Acta Neuropathol Commun 1(1):42
38. Margis R, Margis R, Rieder CR (2011) Identification of blood microRNAs associated to Parkinson s disease. J Biotechnol 152(3):96 101
39. Schipper HM, Maes OC, Chertkow HM, Wang E (2007) MicroRNA expression in Alzheimer blood mononuclear cells. Gene Regul Syst Bio 1:263 274
40. Doleshal M, Magotra AA, Choudhury B, Cannon BD, Labourier E, Szafranska AE (2008) Evaluation and validation of total RNA extraction methods for microRNA expression analyses in formalin-fixed, paraffin-embedded tissues. J Mol Diagn 10(3):203 211
41. Glud M, Klausen M, Gniadecki R, Rossing M, Hastrup N, Nielsen FC, Drzewiecki KT (2009) MicroRNA expression in melanocytic nevi: the usefulness of formalin-fixed, paraffin-embedded material for miRNA microarray profiling. J Invest Dermatol 129(5):1219 1224
42. Lewis F, Maughan NJ, Smith V, Hillan K, Quirke P (2001) Unlocking the archive gene expression in paraffin-embedded tissue. J Pathol 195(1):66 71
43. Liu A, Tetzlaff MT, Vanbelle P, Elder D, Feldman M, Tobias JW, Sepulveda AR, Xu X (2009) MicroRNA expression profiling outperforms mRNA expression profiling in formalin-fixed paraffin-embedded tissues. Int J Clin Exp Pathol 2(6):519 527
44. Szafranska AE, Davison TS, Shingara J, Doleshal M, Riggenbach JA, Morrison CD, Jewell S, Labourier E (2008) Accurate molecular characterization of formalin-fixed, paraffin-embedded tissues by microRNA expression profiling. J Mol Diagn 10(5):415 423
45. Xi Y, Nakajima G, Gavin E, Morris CG, Kudo K, Hayashi K, Ju J (2007) Systematic analysis of microRNA expression of RNA extracted from fresh frozen and formalin-fixed paraffin-embedded samples. RNA 13(10):1668 1674
46. Bing Z, Master SR, Tobias JW, Baldwin DA, Xu XW, Tomaszewski JE (2012) MicroRNA expression profiles of seminoma from paraffin-embedded formalin-fixed tissue. Virchows Arch 461(6):663 668
47. Chen L, Li Y, Fu Y, Peng J, Mo MH, Stamatakos M, Teal CB, Brem RF, Stojadinovic A, Grinkemeyer M, McCaffrey TA, Man YG, Fu SW (2013) Role of deregulated microRNAs in breast cancer progression using FFPE tissue. PLoS One 8(1):e54213
48. Ibusuki M, Fu P, Yamamoto S, Fujiwara S, Yamamoto Y, Honda Y, Iyama K, Iwase H (2013) Establishment of a standardized gene-expression analysis system using formalin-fixed, paraffin-embedded, breast cancer specimens. Breast Cancer 20(2):159 166
49. Lee TS, Jeon HW, Kim YB, Kim YA, Kim MA, Kang SB (2013) Aberrant microRNA expression in endometrial carcinoma using formalin-fixed paraffin-embedded (FFPE) tissues. PLoS One 8(12):e81421
50. Osawa S, Shimada Y, Sekine S, Okumura T, Nagata T, Fukuoka J, Tsukada K (2011) MicroRNA profiling of gastric cancer patients from formalin-fixed paraffin-embedded samples. Oncol Lett 2(4):613 619
51. Penland SK, Keku TO, Torrice C, He X, Krishnamurthy J, Hoadley KA, Woosley JT, Thomas NE, Perou CM, Sandler RS, Sharpless NE (2007) RNA expression analysis of formalin-fixed paraffin-embedded tumors. Lab Invest 87(4):383 391
52. Masuda N, Ohnishi T, Kawamoto S, Monden M, Okubo K (1999) Analysis of chemical modification of RNA from formalin-fixed samples and optimization of molecular biology applications for such samples. Nucleic Acids Res 27(22):4436 4443
53. Vejnar CE, Zdobnov EM (2012) miRmap: Comprehensive prediction of microRNA target repression strength. Nucleic Acids Res 40(22):11673 11683
54. Cowherd RB, Asmar MM, Alderman JM, Alderman EA, Garland AL, Busby WH, Bodnar WM, Rusyn I, Medoff BD, Tisch R, Mayer-Davis E, Swenberg JA, Zeisel SH, Combs TP (2010) Adiponectin lowers glucose production by increasing SOGA. Am J Pathol 177(4):1936 1945
55. Fimia GM, Stoykova A, Romagnoli A, Giunta L, Di Bartolomeo S, Nardacci R, Corazzari M, Fuoco C, Ucar A, Schwartz P, Gruss P, Piacentini M, Chowdhury K, Cecconi F (2007) Ambra1 regulates autophagy and development of the nervous system. Nature 447(7148):1121 1125
56. Zhong Y, Wang QJ, Li X, Yan Y, Backer JM, Chait BT, Heintz N, Yue Z (2009) Distinct regulation of autophagic activity by Atg14L and Rubicon associated with Beclin 1-phosphatidylinositol-3-kinase complex. Nat Cell Biol 11(4):468 476
57. Chan EY, Longatti A, McKnight NC, Tooze SA (2009) Kinase-inactivated ULK proteins inhibit autophagy via their conserved C-terminal domains using an Atg13-independent mechanism. Mol Cell Biol 29(1):157 171
58. Mori F, Tanji K, Miki Y, Wakabayashi K (2009) Decreased cystatin C immunoreactivity in spinal motor neurons and astrocytes in amyotrophic lateral sclerosis. J Neuropathol Exp Neurol 68(11):1200 1206
59. Groelz D, Sobin L, Branton P, Compton C, Wyrich R, Rainen L (2013) Non-formalin fixative versus formalin-fixed tissue: a comparison of histology and RNA quality. Exp Mol Pathol 94(1):188 194
60. von Ahlfen S, Missel A, Bendrat K, Schlumpberger M (2007) Determinants of RNA quality from FFPE samples. PLoS One 2(12):e1261
61. Shi X, Wallis AM, Gerard RD, Voelker KA, Grange RW, DePinho RA, Garry MG, Garry DJ (2012) Foxk1 promotes cell proliferation and represses myogenic differentiation by regulating Foxo4 and Mef2. J Cell Sci 125(Pt 22):5329 5337
62. Liu N, Nelson BR, Bezprozvannaya S, Shelton JM, Richardson JA, Bassel-Duby R, Olson EN (2014) Requirement of MEF2A, C, and D for skeletal muscle regeneration. Proc Natl Acad Sci U S A 111(11):4109 4114
63. Humphries AC, Donnelly SK, Way M (2014) Cdc42 and the Rho GEF intersectin-1 collaborate with Nck to promote N-WASPdependent actin polymerisation. J Cell Sci 127(Pt 3):673 685
64. Tsetsenis T, Younts TJ, Chiu CQ, Kaeser PS, Castillo PE, S?dhof TC (2011) Rab3B protein is required for long-term depression of hippocampal inhibitory synapses and for normal reversal learning. Proc Natl Acad Sci U S A 108(34):14300 14305
65. Carta E, Chung SK, James VM, Robinson A, Gill JL, Remy N, Vanbellinghen JF, Drew CJ, Cagdas S, Cameron D, Cowan FM, Del Toro M, Graham GE, Manzur AY, Masri A, Rivera S, Scalais E, Shiang R, Sinclair K, Stuart CA, Tijssen MA, Wise G, Zuberi SM, Harvey K, Pearce BR, Topf M, Thomas RH, Supplisson S, Rees MI, Harvey RJ (2012) Mutations in the GlyT2 gene (SLC6A5) are a second major cause of startle disease. J Biol Chem 287(34):28975 28985
66. Ajit Bolar N, Vanlander AV, Wilbrecht C, Van der Aa N, Smet J, De Paepe B, Vandeweyer G, Kooy F, Eyskens F, De Latter E, Delanghe G, Govaert P, Leroy JG, Loeys B, Lill R, Van Laer L, Van Coster R (2013) Mutation of the iron-sulfur cluster assembly gene IBA57 causes severe myopathy and encephalopathy. Hum Mol Genet 22(13):2590 2602
67. Rowe GC, Jang C, Patten IS, Arany Z (2011) PGC-1β regulates angiogenesis in skeletal muscle. Am J Physiol Endocrinol Metab 301(1):E155 E163
68. Yang Q, She H, Gearing M, Colla E, Lee M, Shacka JJ, Mao Z (2009) Regulation of neuronal survival factor MEF2D by chaperone-mediated autophagy. Science 323(5910):124 127
69. Francius C, Clotman F (2010) Dynamic expression of the Onecut transcription factors HNF-6, OC-2 and OC-3 during spinal motor neuron development. Neuroscience 165(1):116 129
70. Shen E, Shulha H, Weng Z, Akbarian S (2004) Regulation of histone H3K4 methylation in brain development and disease. Philos Trans R Soc Lond B Biol Sci 369(1652). doi:10.1098/rstb.2013.0514
71. Toriumi K, Ikami M, Kondo M, Mouri A, Koseki T, Ibi D, Furukawa-Hibi Y, Nagai T, Mamiya T, Nitta A, Yamada K, Nabeshima T (2013) SHATI/NAT8L regulates neurite outgrowth via microtubule stabilization. J Neurosci Res 91(12):1525 1532
72. Wilczynska KM, Singh SK, Adams B, Bryan L, Rao RR, Valerie K, Wright S, Griswold-Prenner I, Kordula T (2009) Nuclear factor I isoforms regulate gene expression during the differentiation of human neural progenitors to astrocytes. Stem Cells 27(5):1173 1181

73. Wei J, Fujita M, Nakai M, Waragai M, Watabe K, Akatsu H, Rockenstein E, Masliah E, Hashimoto M (2007) Enhanced lysosomal pathology caused by β-synuclein mutants linked to dementia with Lewy bodies. J Biol Chem 282 (39):28904 28914
74. Wen Y, Zand B, Ozpolat B, Szczepanski MJ, Lu C, Yuca E, Carroll AR, Alpay N, Bartholomeusz C, Tekedereli I, Kang Y, Rupaimoole R, Pecot CV, Dalton HJ, Hernandez A, Lokshin A, Lutgendorf SK, Liu J, Hittelman WN, Chen WY, Lopez-Berestein G, Szajnik M, Ueno NT, Coleman RL, Sood AK (2014) Antagonism of tumoral prolactin receptor promotes autophagy-related cell death. Cell Rep 7(2):488 500
75. Choi AM, Ryter SW, Levine B (2013) Autophagy in human health and disease. N Engl J Med 368(7):651 662
76. Nixon RA, Yang DS (2011) Autophagy failure in Alzheimer s disease locating the primary defect. Neurobiol Dis 43(1):38 45
77. Sasaki S (2011) Autophagy in spinal cord motor neurons in sporadic amyotrophic lateral sclerosis. J Neuropathol Exp Neurol 70(5):349 359
78. Tanji K, Mori F, Kakita A, Takahashi H, Wakabayashi K (2011) Alteration of autophagosomal proteins (LC3, GABARAP and GATE-16) in Lewy body disease. Neurobiol Dis 43(3):690 697
79. Tanji K, Odagiri S, Maruyama A, Mori F, Kakita A, Takahashi H, Wakabayashi K (2012) Alteration of autophagosomal proteins in multiple system atrophy. Neurobiol Dis 49C:190 198
80. Sepe S, Nardacci R, Fanelli F, Rosso P, Bernardi C, Cecconi F, Mastroberardino PG, Piacentini M, Moreno S (2014) Expression of Ambra1 in mouse brain during physiological and Alzheimer type aging. Neurobiol Aging 35(1):96 108
81. Abrahamsen HN, Steiniche T, Nexo E, Hamilton-Dutoit SJ, Sorensen BS (2003) Towards quantitative mRNA analysis in paraffin-embedded tissues using real-time reverse transcriptase-polymerase chain reaction: a methodological study on lymph nodes from melanoma patients. J Mol Diagn 5(1):34 41
82. Peir?-Chova L, Pe?a-Chilet M, L?pez-Guerrero JA, Garc?a-Gim?nez JL, Alonso-Yuste E, Burgues O, Lluch A, Ferrer-Lozano J, Ribas G (2013) High stability of microRNAs in tissue samples of compromised quality. Virchows Arch 463(6):765 774
83. Hui AB, Shi W, Boutros PC, Miller N, Pintilie M, Fyles T, McCready D, Wong D, Gerster K, Waldron L, Jurisica I, Penn LZ, Liu FF (2009) Robust global micro-RNA profiling with formalin-fixed paraffin-embedded breast cancer tissues. Lab Invest 89(5):597 606
84. Hutvagner G, Simard MJ (2008) Argonaute proteins: key players in RNA silencing. Nat Rev Mol Cell Biol 9(1):22 32
85. Mourelatos Z, Dostie J, Paushkin S, Sharma A, Charroux B, Abel L, Rappsilber J, Mann M, Dreyfuss G (2002) miRNPs: a novel class of ribonucleoproteins containing numerous microRNAs. Genes Dev 16(6):720 728
86. Arai T, Hasegawa M, Akiyama H, Ikeda K, Nonaka T, Mori H, Mann D, Tsuchiya K, Yoshida M, Hashizume Y, Oda T (2006) TDP-43 is a component of ubiquitin-positive tau-negative inclusions in frontotemporal lobar degeneration and amyotrophic lateral sclerosis. Biochem Biophys Res Commun 351(3):602 611
87. Neumann M, Sampathu DM, Kwong LK, Truax AC, Micsenyi MC, Chou TT, Bruce J, Schuck T, Grossman M, Clark CM, McCluskey LF, Miller BL, Masliah E, Mackenzie IR, Feldman H, Feiden W, Kretzschmar HA, Trojanowski JQ, Lee VM (2006) Ubiquitinated TDP-43 in frontotemporal lobar degeneration and amyotrophic lateral sclerosis. Science 314(5796):130 133
88. Van Humbeeck C, Cornelissen T, Hofkens H, Mandemakers W, Gevaert K, De Strooper B, Vandenberghe W (2011) Parkin interacts with Ambra1 to induce mitophagy. J Neurosci 31(28):10249 10261
89. Wang IF, Guo BS, Liu YC, Wu CC, Yang CH, Tsai KJ, Shen CK (2012) Autophagy activators rescue and alleviate pathogenesis of a mouse model with proteinopathies of the TAR DNA-binding protein 43. Proc Natl Acad Sci U S A 109(37):15024 15029
90. Zhang X, Li L, Chen S, Yang D, Wang Y, Zhang X, Wang Z, Le W (2011) Rapamycin treatment augments motor neuron degeneration in SOD1^{G93A} mouse model of amyotrophic lateral sclerosis. Autophagy 7(4):412 425

doi:10.1186/s40478-014-0173-z
Cite this article as: Wakabayashi *et al.*: Analysis of microRNA from archived formalin-fixed paraffin-embedded specimens of amyotrophic lateral sclerosis. *Acta Neuropathologica Communications* 2014 2:173.

Submit your next manuscript to BioMed Central and take full advantage of:

- Convenient online submission
- Thorough peer review
- No space constraints or color figure charges
- Immediate publication on acceptance
- Inclusion in PubMed, CAS, Scopus and Google Scholar
- Research which is freely available for redistribution

Submit your manuscript at
www.biomedcentral.com/submit

BioMed Central

NEUROPATHOLOGY

Neuropathology 2014; ••, ••–••

doi:10.1111/neup.12105

Case Report

Bunina bodies in motor and non-motor neurons revisited: A pathological study of an ALS patient after long-term survival on a respirator

Tadashi Kimura,[1] Haishan Jiang,[1] Takuya Konno,[2] Makiko Seto,[3] Keisuke Iwanaga,[3] Mitsuhiro Tsujihata,[3] Akira Satoh,[3] Osamu Onodera,[2] Akiyoshi Kakita[1] and Hitoshi Takahashi[1]

Departments of [1]Pathology and [2]Molecular Neuroscience, Brain Research Institute, University of Niigata, Niigata and [3]Section of Neurology, Nagasaki Kita Hospital, Nagasaki, Japan

Bunina bodies (BBs) are small eosinophilic neuronal cytoplasmic inclusions (NCIs) found in the remaining lower motor neurons (LMNs) of patients with sporadic amyotrophic lateral sclerosis (SALS), being a specific feature of the cellular pathology. We examined a case of SALS, unassociated with *TDP-43* or *C9ORF72* mutation, of 12 years duration in a 75-year-old man, who had received artificial respiratory support for 9 years, and showed widespread multisystem degeneration with TDP-43 pathology. Interestingly, in this patient, many NCIs reminiscent of BBs were observed in the oculomotor nucleus, medullary reticular formation and cerebellar dentate nucleus. As BBs in the cerebellar dentate nucleus have not been previously described, we performed ultrastructural and immunohistochemical studies of these NCIs to gain further insight into the nature of BBs. In each region, the ultrastructural features of these NCIs were shown to be identical to those of BBs previously described in LMNs. These three regions and the relatively well preserved sacral anterior horns (S1 and S2) and facial motor nucleus were immunostained with antibodies against cystatin C (CC) and TDP-43. Importantly, it was revealed that BBs exhibiting immunoreactivity for CC were a feature of LMNs, but not of non-motor neurons, and that in the cerebellar dentate nucleus, the ratio of neurons with BBs and TDP-43 inclusions/neurons with BBs was significantly lower than in other regions. These findings suggest that the occurrence of BBs with CC immunoreactivity is intrinsically associated with the particular cellular properties of LMNs, and that the mechanism responsible for the formation of BBs is distinct from that for TDP-43 inclusions.

Key words: amyotrophic lateral sclerosis, Bunina body, cystatin C, non-motor neuron, TDP-43.

INTRODUCTION

Bunina bodies (BBs), which are small eosinophilic neuronal cytoplasmic inclusions (NCIs), are considered to be a specific feature of the cellular pathology in sporadic amyotrophic lateral sclerosis (SALS). BBs are found in lower motor neurons (LMNs) in the spinal cord and brainstem;[1] Piao *et al.* reported that they were observed in 88 (86.3%) of 102 cases of SALS.[2] However, BBs are very rare in the brainstem and in sacral LMNs innervating the striated muscles of the eye and the rectum and urethral sphincter.[1,3,4] Electron microscopy and immunohistochemical studies are important for identifying BBs in patients with SALS: they consist of electron-dense amorphous material often with inner clear areas containing cell organelles, such as filaments (neurofilaments) and vesicles,[1,2] and are immunoreactive for cystatin C (CC), a protein inhibitor of lysosomal cysteine proteases.[1,5]

In SALS, NCIs indistinguishable from BBs may also occur in non-motor neurons,[1] including those in the medullary reticular formation.[6] The ultrastructural features of such NCIs in non-motor neurons have been shown to be identical to those of BBs seen in LMNs.[1,6] However, no reported studies have yet investigated the immunoreactivity of BBs for CC or their relationship to trans-activation response DNA protein 43 (TDP-43) inclusions.

Recently, we encountered a patient with SALS who had survived for a long period on respirator support. In this patient, many small eosinophilic NCIs reminiscent of BBs,

Correspondence: Hitoshi Takahashi, MD, Department of Pathology, Brain Research Institute, University of Niigata, 1-757 Asahimachi, Chuo-ku, Niigata 951-8585, Japan. Email: hitoshi@bri.niigata-u.ac.jp

Received 16 July 2013; revised and accepted 28 December 2013.

© 2014 Japanese Society of Neuropathology

which were confirmed in the affected LMNs (described below), were observed in the oculomotor nucleus, medullary reticular formation and cerebellar dentate nucleus. Therefore we performed ultrastructural and immunohistochemical studies of these NCIs to gain further insight into the nature of BBs. Here we describe the clinicopathological features of this patient with new observations on Bunina bodies.

CASE REPORT

The present study was conducted with approval from the Institutional Review Board of the University of Niigata. Written informed consent was obtained from the patient's family prior to these genetic studies of the *TDP-43* and *C9ORF72* genes.

Clinical summary and pathological findings

A 63-year-old man became aware of muscle weakness in the right hand, and over the next 2 years, the muscle weakness extended to all of his extremities. On examination, fasciculation was evident in the tongue and deep tendon reflexes were increased; on this basis he was diagnosed as having ALS. About 3 years after onset, at the age of 66 years, he became bedridden with dysphagia and dyspnea, necessitating tube feeding and artificial respiratory support. Thereafter, ocular movement became limited in all directions, making communication impossible. The patient died of bronchopneumonia at the age of 75 years, about 12 years after disease onset. A general autopsy was performed 3 h after death, at which time the brain weighed 830 g, showing marked frontotemporal atrophy (frontal > temporal) (Fig. 1A).

The brain and spinal cord were fixed in 20% buffered formalin and multiple tissue blocks were embedded in paraffin. Histological examination was performed on 4-μm-thick sections using several stains, including HE, KB and Holzer. Selected sections were also immunostained with antibodies against phosphorylated TDP-43 (pTDP-43) (monoclonal, clone S409/410; Cosmo Bio, Tokyo, Japan; 1:3000, heat/autoclaving) and cystatin C (polyclonal, Dako, Glostrup, Denmark; 1:3000).

The entire spinal cord was markedly atrophic (Fig. 1B) and there was severe wasting in the anterior nerve roots. Histopathological examination revealed that except for the absence of Lewy body-like hyaline inclusions, the entire pathological picture was very similar to that shown in a case of SALS in a 71-year-old woman after long-term survival on a respirator, which we had previously reported.[7] With regard to the motor neuron system, almost complete loss of LMNs was observed in the spinal anterior horns at the levels of the cervical, thoracic and lumbar segments. The sacral anterior horns (S1 and S2), including Onuf's nucleus, contained a number of LMNs (Fig. 1C). In the brainstem, almost complete loss of LMNs was evident in the hypoglossal nucleus. The facial motor nucleus and oculomotor nucleus were relatively well preserved. BBs were found in the remaining LMNs in the sacral anterior horns, including Onuf's nucleus and the facial motor nucleus (Fig. 1D); immunostaining revealed that these BBs were

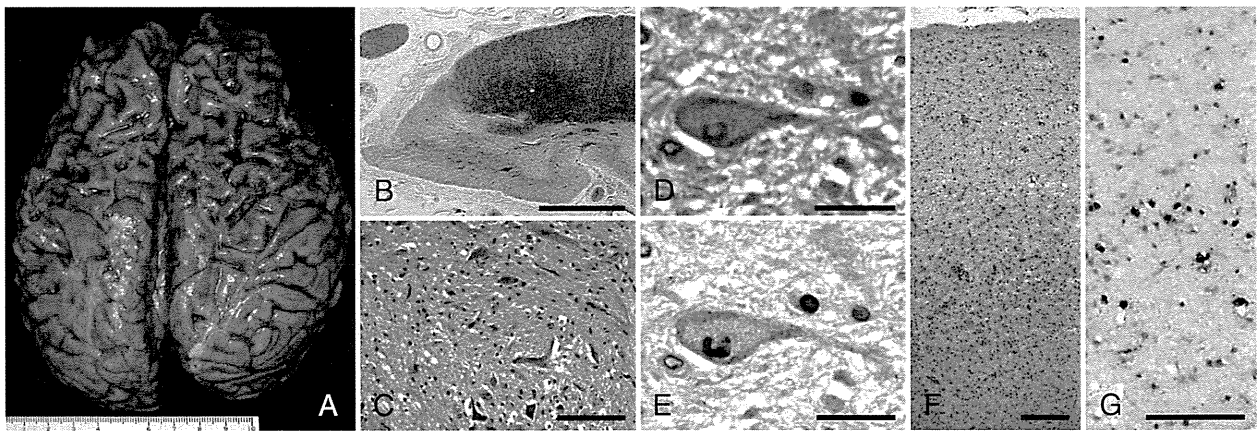

Fig. 1 Neuropathological findings in the brain and spinal cord. Sections stained by the KB method (B), HE (C,D,F) and immunostained with antibodies against cystatin C (CC) (E) and phosphorylated trans-activation response DNA protein 43 (pTDP43) (G). (A) Marked atrophy is evident in the frontal lobe, including the precentral gyrus. (B) The thoracic segment (T2), showing myelin pallor in the white matter except for the posterior columns. (C) Loss of lower motor neurons (LMNs) with gliosis is evident in the sacral (S1) anterior horn. Note that Onuf's nucleus contains a number of LMNs (lower). (D,E) Sequential staining of the same section, showing two facial motor neurons with Bunina bodies (BBs) (D) positive for CC (E). (F) Severe neuronal loss with gliosis is evident in the motor cortex. (G) Here, pTDP-43-positive neuronal cytoplasmic inclusions (NCIs) in layers II-III are shown. Scale bars = 1 mm for (B), 100 μm for (C,G), 20 μm for (D,E) and 200 μm for (F).

© 2014 Japanese Society of Neuropathology

positive for CC (Fig. 1E). In the motor cortex, severe neuronal loss was also evident and no Betz cells were found (Fig. 1F); immunostaining revealed pTDP-43-positive NCIs mainly in layers II-III and V-VI (Fig. 1G). The histological findings are summarized in Table 1. Diffuse loss of cerebellar Purkinje cells appeared to be attributable to brain ischemia (Table 1).

Table 1 Pathological findings in the present case

Regions	Loss of neuron	pTDP-43-positive NCIs
Cerebral cortex		
Frontal	+++	+++
Motor	+++	+++
Parietal	++	+++
Cingulate	+++	+++
Insular	+++	+++
Entorhinal	++	+++
Hippocampus (DG/Sub)	+/+++	+++/++
Subcortical area		
Amygdala	++	+++
Basal nucleus of Mynert	+	+
Caudate nuclei	+++/+++	+++/+++
Globus pallidus	+	+++
Thalamus (medial/lateral)	++/+++	++/++
Subthalamic nucleus	nd	nd
Midbrain		
Midbrain tectum	+++	+++
Reticular formation	+++	+++
Oculomotor nucleus	+	+
Red nucleus	+	+
Substance nigra	+++	+
Pons		
Locus celreus	++	+
Reticular formation	++	+++
Facial nucleus (motor)	+	++
Vestibular nucleus	+	+
Pontine nucleus	+	++
Superior olivary nucleus	–	–
Medulla oblongata		
Hypoglossal nucleus	+++	–
Dorsal vagal nucleus	+	++
Reticular formation	++	+++
Nucleus ambiguus	nd	nd
Inferior olivary nucleus	+	+
Cerebellum		
Purkinje cell	+++	–
Granule cell	–	–
Dentate nucleus	+	++
Spinal cord		
Anterior horn	+++	+
Intermediate lateral nucleus	++	++
Clarke's nucleus	+++	–
Posterior horn	++	++
Anterior olfactory nucleus	++	++
Dorsal root ganglia	+	+

Loss of neurons: +, mild; ++, moderate; +++, severe. The numbers of pTDP-43-positive neuronal cytoplasmic inclusions (NCIs) were assessed using a semi-quantitative rating scale: –, absent or nearly absent; +, sparse; ++, moderate; +++, numerous. Hippocampus: DG, dentate gyrus (granule cells); Sub, subiculum. nd, not determined.

© 2014 Japanese Society of Neuropathology

TDP-43 mutation and *C9ORF72* repeat expansion analyses

Genomic DNA was prepared from a frozen sample of cerebral cortex from the patient, and then examinations for *TDP-43* mutation and *C9ORF72* repeat expansion were carried out as previously described;[8,9] however, neither of these features was found to be present.

Bunina bodies in motor and non-motor neurons

In addition, the occurrence of many eosinophilic NCIs indistinguishable from BBs in the oculomotor nucleus, medullary reticular formation and cerebellar dentate nucleus was a feature of the present patient. Some representative inclusions in the oculomotor nucleus and medullary reticular formation were recycled for electron microscopy, and small tissue blocks from the formalin-fixed cerebellar dentate nucleus were also processed for ordinary electron microscopy. All of the studied NCIs, 2–3 in each region (Fig. 2A–C), were identified as BBs from their characteristic ultrastructural features (Fig. 2D–F). In the medullary reticular formation, the BB-containing neurons were distributed more widely than previously recorded.[6]

We then investigated the presence or absence of CC immunoreactivity in the BBs, as well as the correlation between the occurrence of BBs and that of pTDP-43-positive inclusions. Four-micrometer-thick paraffin sections that contained the bilateral oculomotor nuclei and medullary reticular formation, and unilateral cerebellar dentate nucleus were prepared, and then stained with HE, observed and photographed (Fig. 3A–C,G–I). They were then destained in absolute ethanol and finally immunostained for CC (Fig. 3D–F) or pTDP-43 (Fig. 3J–L). For comparison, the bilateral sacral anterior horns (S1 and S2) and facial motor nuclei were also similarly examined. The degrees of cytoplasmic staining intensity for CC were generally decreased in the LMNs containing BBs (Fig. 1E,3D–F). pTDP-43-positive NCIs appeared as fine to coarse granular (Fig. 3J), linear wisp-like, large irregular (Fig. 3K) or small round-to-oval inclusions (Fig. 3L); the small round-to-oval inclusions were often observed in neurons in the cerebellar dentate nucleus (Fig. 3L). In each region, the ratio of neurons containing CC-positive BBs to the total cell count of neurons containing BBs was calculated in one section. Similarly, the ratio of neurons containing both BBs and pTDP-43-positive inclusions to the total cell count of neurons containing BBs was calculated in one section. The results obtained are shown in Table 2.

DISCUSSION

Based on the distribution and severity of neuron loss and TDP-43 inclusions, the present case was considered to be

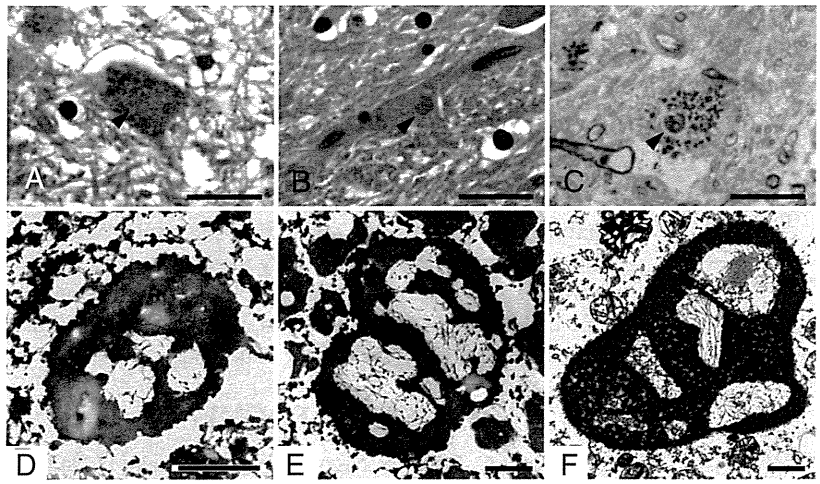

Fig. 2 Ultrastructural profiles of Bunina bodies (BBs) in neurons from the oculomotor nucleus (A), medullary reticular formation (B) and cerebellar dentate nucleus (C). Two paraffin sections stained with HE (A,B) and one Epon section stained with toluidine blue (C). Electron microscopy shows that all the BBs (A–C; arrowheads) have essentially the same ultrastructural profiles, appearing as electron-dense amorphous material with inner clear areas, in which filamentous structures are evident (D–F). In a Bunina body shown in (C), some of the filamentous structures can be identified as neurofilaments, or short fragments of the rough endoplasmic reticulum (F). Scale bars = 20 μm for A–C and 1 μm for D–F.

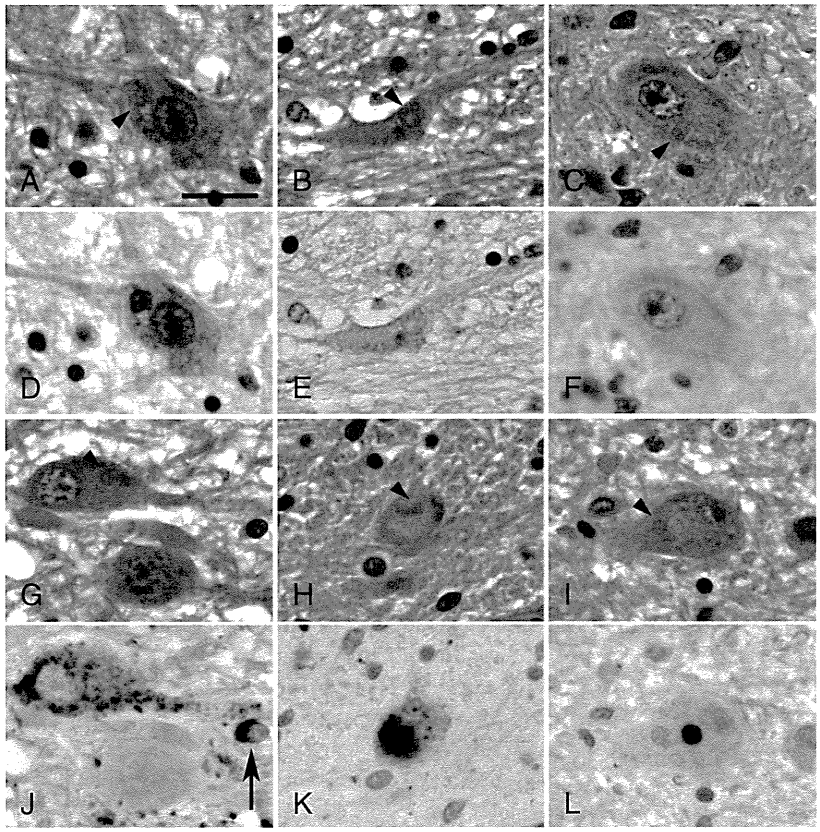

Fig. 3 Immunohistochemical profiles of Bunina bodies (BBs) in neurons from the oculomotor nucleus (A,G), medullary reticular formation (B,H) and cerebellar dentate nucleus (C,I). Sequential staining of the same sections with HE (A–C) and anti-cystatin C (CC) antibody (D–F), as well as with HE (G–I) and anti-phosphorylated trans-activation response DNA protein 43 (pTDP43) antibody (J–L). (A–F) BBs (arrowheads) seen in one lower motor neuron (A) and two non-motor neurons (B,C) are positive (D) and negative (E,F) for CC, respectively. (G–L) In all of the neurons, coexistence of BBs (arrowheads) and pTDP-43-positive neuronal cytoplasmic inclusions (NCIs) is evident; BBs themselves are negative for pTDP-43 (G,J; H,K; I,L). Arrow indicates cytoplasm of a glial cell positive for pTDP-43 (J). Scale bar = 20 μm for (A–L).

an additional example of SALS whose course had been extended by artificial respiratory support, showing widespread multisystem degeneration with TDP-43 pathology (Table 1) (Nishihira *et al.*, Type 2;[10] frontotemporal lobar degeneration – TDP pathology, Type B[11]). We reviewed seven cases in which artificial respiratory support had been used (disease duration, >10 years; Type 1 = 5, Type 2 = 2[10]) and found no NCIs indistinguishable from BBs in the oculomotor nucleus, medullary reticular formation or cerebellar dentate nucleus. In the case (disease duration = $8^2/_3$ years) reported by Nishihira *et al.*,[7] only one BB, which was confirmed by electron microscopy of recycled material, was found in the medullary reticular formation (data not shown). Therefore, the present case, which lacked *TDP-43*

© 2014 Japanese Society of Neuropathology

Table 2 Summary of pathological findings for Bunina bodies (BBs)

Region	Ratio (cystatin C)	Ratio (pTDP-43)
Sacral anterior horn	0.88 (7/8)	1.00 (5/5)
Facial motor nucleus	1.00 (8/8)	0.90 (9/10)
Oculomotor nucleus	1.00 (10/10)	1.00 (13/13)
Medullary reticular formation	0.17 (2*/12)†	0.77 (10/13)
Cerebellar dentate nucleus	0.00 (0/36)†	0.33 (12/ /36)††

Ratio (cystatin C): neurons with cystatin C-positive BBs/neurons with BBs; Ratio (pTDP-43): neurons with BBs and pTDP-43-positive inclusions/neurons with BBs. *Regarded as weakly positive. †$P < 0.01$ versus. sacral anterior horn, facial motor nucleus or oculomotor nucleus. ††$P < 0.05$ versus sacral anterior horn, and $P < 0.01$ versus facial motor nucleus, versus oculomotor nucleus or versus medullary reticular formation. Statistical analyses were performed by Ryan's multiple comparison tests using R software (http://www.r-project.org/).

or *C9OLF72* mutation, appeared to be very unusual in terms of the occurrence of BBs even among cases of SALS whose course had been extended by artificial respiratory support.

At present, TDP-43 is widely recognized to be the pathological protein in SALS.[10,12] BBs have been reported to be negative for TDP-43,[12] which was also confirmed in the present study using a monoclonal antibody against pTDP-43. However, the presence of both BBs and TDP-43-positive NCIs has also been shown to be a characteristic feature of ALS with *TDP-43* mutations,[8,12] emphasizing anew the significance of BBs as a specific feature of the cellular pathology of ALS.

Importantly, the present case is the first reported example in which the presence of BBs exhibiting immunoreactivity for CC was a feature of LMNs, but not of non-motor neurons (Table 2). At the ultrastructural level, it is noteworthy that in LMNs, the electron-dense material considered to represent BBs themselves is negative for CC;[5,13] it has been reported that CC immunoreactivity is markedly decreased in the spinal LMNs in SALS, and that the formation of TDP-43 inclusions, but not BBs, may be linked to the CC content of these LMNs.[13] Based on the present findings, we consider that the occurrence of BBs showing CC immunoreactivity is a phenomenon confined almost exclusively to LMNs, and that this must be associated with the particular cellular properties that characterize the LMNs themselves.

The present case is also the first reported to have demonstrated BBs in neurons in the cerebellar dentate nucleus. It has been reported that there is a significant positive correlation between the occurrence of BBs and that of TDP-43 inclusions in spinal and brainstem LMNs.[14,15] This also appears to be the case in the medullary reticular formation (Table 2). However, the ratio (pTDP-43) was significantly lower in the cerebellar dentate nucleus than in other regions (Table 2), indicating that the mechanism responsible for the formation of BBs is distinct from that for TDP-43 inclusions.

Finally, even though the present study involved only a single case and revealed negativity for BBs, as in other similar cases of SALS mentioned above, the results obtained are of considerable interest. In conclusion, the nature and origin of BBs still remain uncertain. When considering why LMNs are generally most vulnerable in ALS, further studies on the formation of BBs in association with the cellular molecular properties of LMNs are needed to elucidate the pathomechanism underlying the disease.

ACKNOWLEDGMENTS

We thank C. Tanda, S. Nigorikawa, J. Takasaki, H. Saito, T. Fujita and S. Egawa for their technical assistance. This work was supported by a Grant-in-Aid, 23240049, for Scientific Research from the Ministry of Education, Culture, Sports, Science and Technology, and a Grant-in-Aid from the Research Committee for CNS Degenerative Diseases, the Ministry of Health, Labour and Welfare, Japan.

REFERENCES

1. Okamoto K, Mizuno Y, Fujita Y. Bunina bodies in amyotrophic lateral sclerosis. *Neuropathology* 2008; **28**: 109–115.
2. Piao YS, Wakabayashi K, Kakita A *et al.* Neuropathology with clinical correlations of sporadic amyotrophic lateral sclerosis: 102 autopsy cases examined between 1962 and 200. *Brain Pathol* 2003; **12**: 10–22.
3. Okamoto K, Hirai S, Amari M, Iizuka T, Watanabe M, Murakami N. Oculomotor nuclear pathology in amyotrophic lateral sclerosis. *Acta Neuropathol* 1993; **85**: 458–462.
4. Okamoto K, Hirai S, Ishiguro K, Kawarabayashi T, Takatama M. Light and electron microscopic and immunohistochemical observations of the Onuf's nucleus of amyotrophic lateral sclerosis. *Acta Neuropathol* 1991; **81**: 610–614.
5. Okamoto K, Hirai S, Amari M, Watanabe M, Sakurai A. Bunina bodies in amyotrophic lateral sclerosis immunostained with rabbit anti-cystatin C serum. *Neurosci Lett* 1993; **162**: 125–128.
6. Nakano I, Iwatsubo T, Hashizume Y, Mizutani T. Bunina bodies in neurons of the medullary reticular formation in amyotrophic lateral sclerosis. *Acta Neuropathol* 1993; **85**: 471–474.
7. Nishihira Y, Tan CF, Toyoshima Y *et al.* Sporadic amyotrophic lateral sclerosis: widespread multisystem degeneration with TDP-43 pathology in a patient after long-term survival on a respirator. *Neuropathology* 2009; **29**: 689–696.

© 2014 Japanese Society of Neuropathology

8. Yokoseki A, Shiga A, Tan CF *et al.* TDP-43 mutation in familial amyotrophic lateral sclerosis. *Ann Neurol* 2008; **63**: 538–542.
9. Konno T, Shiga A, Tsujino A *et al.* Japanese amyotrophic lateral sclerosis patients with GGGGCC hexanucleotide repeat expansion in *C9ORF72*. *J Neurol Neurosurg Psychiatry* 2013; **84**: 398–401.
10. Nishihira Y, Tan CF, Onodera O *et al.* Sporadic amyotrophic lateral sclerosis: two pathological patterns shown by analysis of distribution of TDP-43-immunoreactive neuronal and glial cytoplasmic inclusions. *Acta Neuropathol* 2008; **116**: 169–182.
11. Mackenzie IR, Neumann M, Baborie A *et al.* A harmonized classification system for FTLD-TDP pathology. *Acta Neuropathol* 2011; **122**: 111–113.
12. Tan CF, Eguchi H, Tagawa A *et al.* TDP-43 immunoreactivity in neuronal inclusions in familial amyotrophic lateral sclerosis with or without SOD1 gene mutations. *Acta Neuropathol* 2007; **113**: 535–542.
13. Mori F, Tanji K, Miki Y, Wakabayashi K. Decreased cystatin C immunoreactivity in spinal motor neurons and astrocytes in amyotrophic lateral sclerosis. *J Neuropathol Exp Neurol* 2009; **68**: 1200–1206.
14. Mori F, Tanji K, Miki Y, Kakita A, Takahashi H, Wakabayashi K. Relationship between Bunina bodies and TDP-43 inclusions in spinal anterior horn in amyotrophic lateral sclerosis. *Neuropathol Appl Neurobiol* 2010; **36**: 345–352.
15. Mori F, Kakita A, Takahashi H, Wakabayashi K. Co-localization of Bunina bodies and TDP-43 inclusions in lower motor neurons in amyotrophic lateral sclerosis. *Neuropathology* 2013. doi:10.1111/neup.12044

© 2014 Japanese Society of Neuropathology

Neuropathology and Applied Neurobiology (2014), **40**, 783–788 doi: 10.1111/nan.12157

Scientific correspondence

C9ORF72 repeat-associated non-ATG-translated polypeptides are distributed independently of TDP-43 in a Japanese patient with c9ALS

Hexanucleotide (GGGGCC) repeat expansion in a noncoding region of *C9ORF72* is the major genetic cause of frontotemporal dementia and amyotrophic lateral sclerosis (c9FTD/ALS) in the Caucasian population [1], but it is very rare in the Japanese population, possibly because of the difference in genetic background [2,3]. TDP-43 pathology indistinguishable from that of non-mutational ALS/FTLD-TDP has been observed in c9FTD/ALS [4]. In addition, the presence of p62-, ubiquitin- and ubiquilin-positive, and TDP-43-negative inclusions in the cerebellar cortex and hippocampus has been reported to be a unique and consistent feature in Caucasian patients with c9FTD/ALS [5,6]. Recently, it was demonstrated that these TDP-43-negative inclusions are derived from aggregated dipeptide repeat (DPR) proteins bidirectionally translated from the expanded repeat in *C9ORF72* by repeat associated non-ATG (RAN) translation, and that such DPR protein pathology is widely distributed in the central nervous system (CNS) [7,8]. However, it still remains unknown whether these distinct neuropathological features are also reproduced in Japanese patients with c9FTD/ALS. In the present study, we performed an immunohistochemical analysis focusing especially on DPR proteins in a Japanese patient with *C9ORF72* repeat expansion (c9ALS) [2], who to our knowledge represents the only autopsy case of this genetic disease to have been reported in the Japanese population so far.

The present study was conducted with approval from the Institutional Review Board of Niigata University. The clinical and pathological findings in this case have been reported previously (case 4 [9]). Briefly, the patient had a sibling who had also been diagnosed as having ALS. At the age of 61, he noticed hand clumsiness, and progressively developed bulbar palsy and limb weakness. He died 20 months after disease onset due to respiratory failure. He had no clinical features suggestive of dementia. The presence of *C9ORF72* repeat expansion was confirmed by repeat-primed PCR using the frozen cerebellar tissue [2]. The accurate hexanucleotide repeat length was unknown, because we could not perform Southern blot analysis due to lack of the amount of genomic DNA. Histologically, neuronal loss and gliosis were evident in the spinal anterior horns, brainstem motor nuclei and motor cortex, as well as degeneration in the anterior and lateral columns of the spinal cord. Bunina bodies and ubiquitin-positive skein-like inclusions were observed in the remaining lower motor neurones. Neuronal and glial (oligodendrocytic) cytoplasmic inclusions (NCIs and GCIs) recognized with anti-TDP-43 (polyclonal, Protein Tec Group, Chicago, IL, USA; 1:4000) were present in the lower motor nuclei and motor cortex, and much less frequently in the subcortical non-motor nuclei, such as the basal ganglia, whereas no such NCIs or GCIs were observed in the cerebellar cortex and hippocampus [9]. There were p62-positive and TDP-43-negative NCIs in the cerebellar granule cells and in the granule cells and pyramidal CA4-CA2 neurones of the hippocampus; at that time, we failed to show phosphorylated TDP-43 (pTDP-43)-positive NCIs in the lower motor nuclei and motor cortex [2].

In the present study, we confirmed that NCIs and GCIs recognized with a 'polyclonal' antibody against pTDP-43 (pS409/410; Cosmo Bio, Tokyo, Japan; 1: 1000) were present with the same distribution pattern as that of TDP-43 mentioned above (Figure 1**a**,**c**). Immunostaining with an antibody against another RNA-binding protein, RNA-binding motif 45 (RBM45) (polyclonal, Sigma-Aldrich, St. Louis, MO, USA; 1:50), which has been known to accumulate in inclusions in ALS [10], also revealed a distribution of positive inclusions strikingly similar to that of TDP-43-positive inclusions, although such NCIs and GCIs were comparatively small in number. The characteristic morphologies of NCIs and GCIs were shared by both anti-TDP-43/anti-pTDP-43 and anti-RBM45 (Figure 1**a**–**d**).

We generated polyclonal antibodies against putative DPR proteins from the GGGGCC repeat by RAN translation [11]. Although immunostaining with three antibodies against different polypeptides, poly Gly-Ala (GA), poly Gly-Pro and poly Gly-Arg, arising from RAN translation revealed similar DPR protein pathology, abundant positive

© 2014 British Neuropathological Society

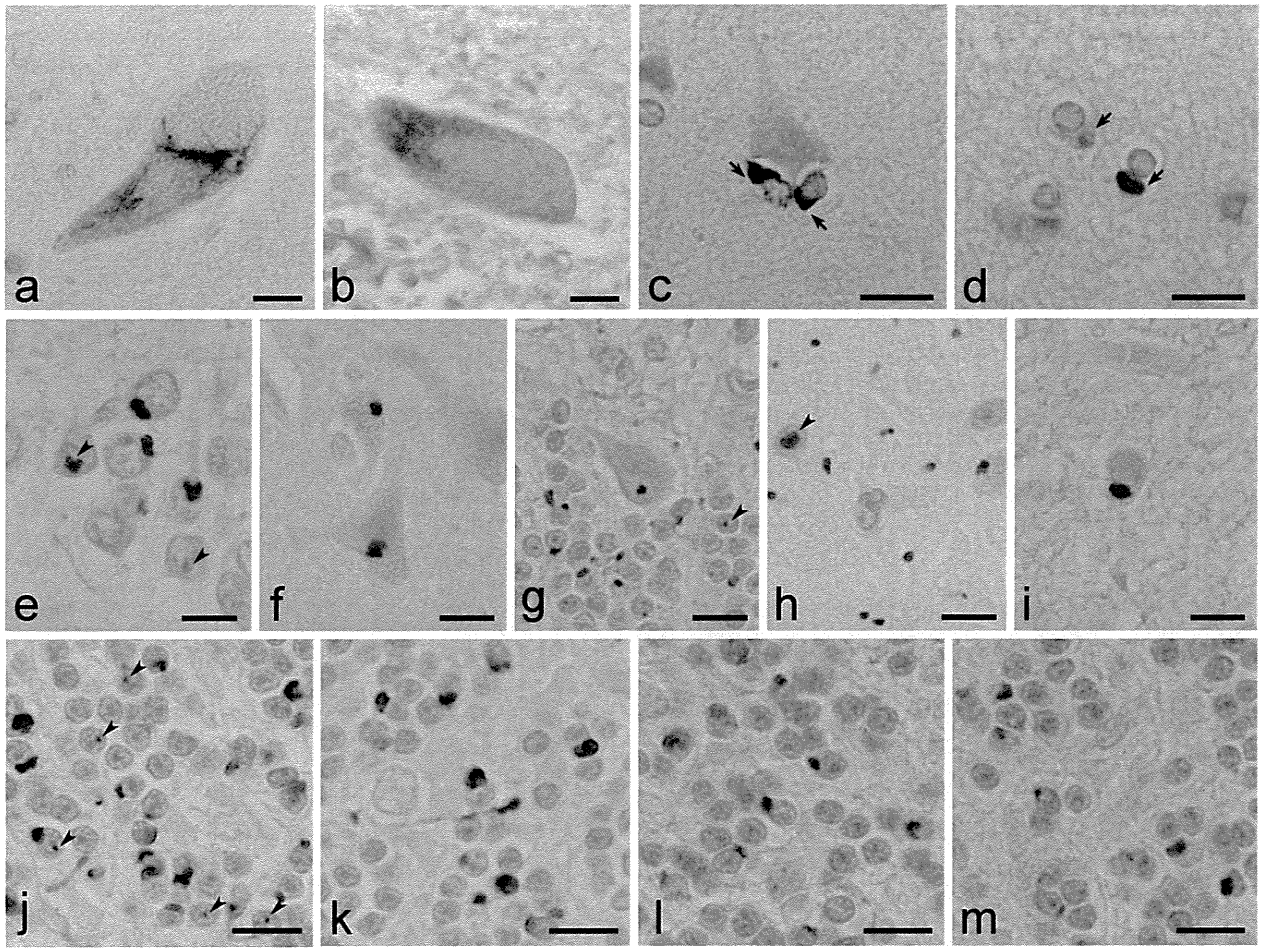

Figure 1. Immunohistochemical study. (**a**–**d**) Skein-like cytoplasmic inclusions positive for phosphorylated TDP-43 (pTDP-43) (**a**) and RBM45 (**b**) in the cervical anterior horn cells. C-like or fibrillary tangle-like glial cytoplasmic inclusions positive for pTDP-43 (**c**) and RBM45 (**d**) in the motor cortex. Note glial cytoplasmic inclusions indicated by arrows (**c**,**d**). (**e**–**h**) Numerous poly Gly-Ala (GA)-positive neuronal cytoplasmic and intranuclear inclusions (arrowheads) are observed widely beyond the regions showing TDP-43-positive inclusions [(**e**) hippocampal dentate gyrus, (**f**) temporal cortex, (**g**) cerebellar granular-Purkinje layer, (**h**) cerebellar molecular layer; also see Table 1]. A Purkinje cell also contains a positive cytoplasmic inclusion (**g**). Punctate or linear inclusions in the neuropil of the cerebellar molecular layer are also evident (**h**). (**i**) Here, an oligodendroglial cytoplasmic inclusion is shown in the precentral subcortical white matter. (**j**–**m**) In the cerebellar granular layer, it is evident that GA-positive neuronal cytoplasmic inclusions (**j**) are also positive for ubiquilin (**k**), ubiquitin (**l**) and p62 (**m**). Note GA-positive intranuclear inclusions indicated by arrowheads (**j**). Bars: 10 μm (**a**–**m**).

inclusions were recognized most clearly with anti-poly GA (1:1000). The distribution pattern of DPR protein-positive NCIs was apparently different from that of TDP-43-positive NCIs, the latter being clearly associated with neuronal loss in the lower and upper motor neurones systems. DPR protein-positive NCIs were widely distributed in the brain (Figure 1**e**–**h**,**j**), with the highest frequency in the hippocampal dentate gyrus (Figure 1**e**) and cerebellar granular layer (Figure 1**g**,**j**), and were distributed almost evenly in the cerebral neocortex examined (Figure 1**f**). DPR protein-positive GCIs were comparatively rare (Figure 1**i**), although TDP-43- and RBM45-positive GCIs were observed frequently (Figure 1**c**,**d**). Neuronal intranuclear inclusions were frequently associated with anti-DPR proteins (Figure 1**e**,**g**,**h**,**j**), but not with anti-TDP-43. DPR protein-positive punctate or filamentous structures were also encountered in the neuropil of the cerebellar molecular layer (Figure 1**h**), which were never recognized with anti-TDP-43, and only rarely with anti-ubiquilin (monoclonal, clone 5F5, Abnova, Walnut, CA, USA; 1:10 000). DPR protein-positive NCIs appeared as irregular dot-like, granular or star-like inclusions

© 2014 British Neuropathological Society